

**REALISTIC MODELLING OF CHIPLESS RFID BASED
MULTI-SENSOR TAG**



by

NS Momina Nadeem

00000328535/MSEE26

Supervisor

Assoc Prof Mir Yasir Umair, PhD

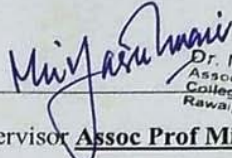
Co-Supervisor

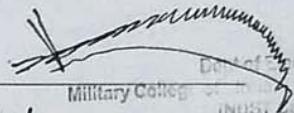
Asst Prof Ayesha Habib, PhD

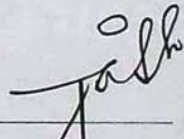
A thesis submitted to the faculty of Electrical Engineering Department Military
College of Signals, National University of Sciences and Technology,
Rawalpindi as part of the requirements for the degree of MS in
Electrical Engineering
OCT 2023

THESIS ACCEPTANCE CERTIFICATE

Certified that final copy of MS/MPhil thesis written by Miss **NS Momina Nadeem** Registration No. **00000328535** of **Military College of Signals** has been vetted by undersigned, found complete in all respect as per NUST Statutes/Regulations, is free of plagiarism, errors and mistakes and is accepted as partial, fulfillment for award of MS/MPhil degree. It is further certified that necessary amendments as pointed out by GEC members of the student have been also incorporated in the said thesis.

Signature: 
Dr. Mir Yasir Umair
Associate Professor
College of Signals, NUST
Rawalpindi
Name of Supervisor **Assoc Prof Mir Yasir Umair, PhD**
Date: 19/10/23

Signature (HoD): 
Brig
HoD
Dept of Elec Engrg
Military College of Signals (NUST)
(NUST, Campus)
Date: 19/10/23

Signature (Dean): 
Date: 23/10/23
Brig
Dean, MCS (NUST)
(Asif Masood, PhD)

DECLARATION

I affirm that the work "Realistic Modelling of Chipless RFID based Multi-sensor Tag" presented in this thesis was not submitted in support of any other prize or academic credential, either at this school or elsewhere.

DEDICATION

This thesis is dedicated to

MY BELOVED PARENTS, HONORABLE TEACHERS AND

FRIENDS for their love, endless support, and

encouragement

Abstract

Radio Frequency Identification (RFID) is one of the leading supporting technologies for Internet-of-Things (IoT) allowing data from everyday objects to be collected and shared via internet. RFID technology was developed to overcome the short comings of the conventional optical object recognition methods like barcodes which required line-of-sight communication, human intervention, closer reading range and it could scan only one object at a time. RFID technology avoids all these limitations by providing a non-line-of-sight communication at a faster speed, greater reading range and without any physical contact, multiple objects can be detected remotely and simultaneously.

Today, RFID finds vast applications in various sectors that include retail and logistics, healthcare, food and pharmaceutical industry, agriculture, transport, security, etc. for purposes like access control, inventory and asset tracking, parking, theft control, environmental monitoring, etc. Keeping in view the increasing demand of fast identification and tracking of objects without requiring direct line-of-sight, an RFID tag has been proposed in this research that has a compact dimension and offers a high data density. The reported tag is a chipless RFID based multi-sensor tag that can act both as a humidity sensor or a temperature sensor. The tag has a slot-resonator-based geometry and occupies a miniscule area of 2.4 cm^2 with data transmission capacity of 29 bits. The tag has initially been designed using Rogers RT/duroid[®] 5880 which operates in the frequency range of 5.48 – 28.87 GHz. The same tag has been optimized for four other rigid and flexible substrates that include Rogers RT/duroid[®] 5870, Taconic TLX-0 Kapton[®]HN and PET (Polyethylene Terephthalate) using copper, Aluminium and silver nano-particle-based ink as radiators. Integration of sensing feature within the same tag has been achieved by the deployment of a thin film of Kapton[®]HN over the longest slot of the tag for moisture sensing, and filling of Stanyl[®] Polyamide in the longest slot for temperature sensing. The sensing behavior of the tag is exhibited in the Most Significant Bit (MSB) in the microwave response of the tag. The novelty of the tag lies in its ability to tag $2^{29} = 536,870,912$ distinct objects, its flexibility, printability, high code density of 12.08 bits/cm^2 , and sensing property.

ACKNOWLEDGEMENTS

All praise belongs to the Powerful Allah, who has given me the courage and resilience to accomplish my objectives. First of all, I would like to express my sincere gratitude to my Supervisor Dr. Mir Yasir Umair and my devoted and respectful co-supervisor Dr. Ayesha Habib for their assistance, cooperation, and direction during the course of my thesis. They generously offered to supervise me as I worked on my thesis and greatly assisted me in finishing my study. Additionally, I would like to express my gratitude to my committee members for their assistance and insightful comments on my study. Last but not least, I would like to thank my parents and siblings, to whom I am dedicating this effort, from the bottom of my heart. Without their generous assistance, prayers, and encouragement, this thesis would not be possible.

TABLE OF CONTENTS

THESIS ACCEPTANCE CERTIFICATE	2
DECLARATION.....	3
DEDICATION	4
ABSTRACT	5
ACKNOWLEDGEMENTS	6
TABLE OF CONTENTS.....	7
LIST OF TABLES	10
LIST OF FIGURES	11
ACRONYMS	13
<i>Chapter 1 – INTRODUCTION.....</i>	14
1.1 History of RFID	14
1.2 Internet-of-Things (IoT).....	15
1.3 Printed Electronics	16
1.4 RFID Technology	16
1.5 Types of RFID Systems.....	17
1.5.1 LF RFID.....	17
1.5.2 HF RFID	18
1.5.3 NFC	19
1.5.4 UHF RFID.....	19
1.6 Classification of RFID Tags	19
1.6.1 Active RFID Tags	20
1.6.2 Passive RFID Tags.....	21
1.6.3 Semi-Passive RFID Tags.....	22
1.7 Coupling Mechanisms.....	23
1.7.1 Inductive Coupling.....	23
1.7.2 Backscatter Coupling	24
1.7.3 Transmitter Type Coupling	25
1.7.4 Transponder Type Coupling.....	26

1.8 Applications of RFID Technology	26
1.8.1 Retail	26
1.8.2 Logistics and Supply Chain Management	27
1.8.3 Healthcare	27
1.8.4 Manufacturing	27
1.8.5 Automotive Industry	27
1.8.6 Hospitality and Events.....	27
1.8.7 Agriculture and Livestock	28
1.9 Sensor Integration	28
1.10 Objectives	28
1.11 Organization of Thesis.....	29
Chapter 2 – LITERATURE REVIEW	30
Chapter 3 – PROPOSED CHIPLESS RFID TAG.....	38
3.1 Fundamental Operation of the Tag	38
3.2 Development of the Proposed Tag	40
3.2.1 Surface Current Distribution.....	43
3.3 Humidity Sensor.....	44
3.4 Temperature Sensor	46
Chapter 4 – RESULTS AND DISCUSSIONS	48
4.1 Proposed Tag Analysis	48
4.1.1 Tag-A	48
4.1.2 Tag-B	49
4.1.3 Tag-C	49
4.1.4 Tag-D.....	50
4.1.5 Tag-D'	50
4.1.6 Tag-E	51
4.1.7 Tag-E'	52
4.1.8 Comparison of the Tags Designed	53

4.2	Experimental Setup	54
4.3	Multiple ID Combination	56
4.4	Humidity Sensing Behavior of the Tag	57
4.5	Temperature Sensing Behavior of the Tag	59
4.6	Comparison with Previously Published RFID Tags.....	62
Chapter 5 – CONCLUSION		63
5.1	Conclusion	63
5.2	Trends in the RFID Market for 2023 and Beyond: A Five-Year Outlook	64
5.3	Future Work.....	66
Chapter 6 – BIBLIOGRAPHY		68
List of Publications		75

LIST OF TABLES

Table 1	Dimensions of the slot resonator structure	42
Table 2	Comparison table for the designed tags using different substrates	53
Table 3	Comparison of the reported tag with previously reported tags	62

LIST OF FIGURES

Fig 1.1	RFID taking IoT to widespread applications	15
Fig 1.2	A commercial active RFID Tag.....	20
Fig 1.3	Passive RFID tag.....	21
Fig 1.4	A semi-passive RFID Tag	22
Fig 1.5	An RFID system with inductive coupling.....	24
Fig 1.6	An RFID system with backscatter coupling.....	25
Fig 2.1	Design and RCS response of the tag presented in [18]	30
Fig 2.2	Design and RCS response of the tag presented in [19]	31
Fig 2.3	Design and RCS response of the tag presented in [20]	31
Fig 2.4	Design and RCS response of the tag presented in [21]	32
Fig 2.5	Design and RCS response of the tag presented in [22]	32
Fig 2.6	Design and RCS response of the tag presented in [23]	33
Fig 2.7	Design and RCS response of the tag presented in [24]	34
Fig 2.8	Design and RCS response of the tag presented in [25]	34
Fig 2.9	Design and RCS response of the tag presented in [26]	35
Fig 2.10	Design and RCS response of the tag presented in [27]	35
Fig 2.11	Design and RCS response of the tag presented in [28]	36
Fig 2.12	Design and RCS response of the tag presented in [29]	36
Fig 2.13	Design and RCS response of the tag presented in [30]	37
Fig 3.1	Backscattering phenomenon in chipless RFID tags.....	39
Fig 3.2	Arrangement of tag in simulation setup.....	40
Fig 3.3	Layout of the proposed tag	41
Fig 3.4 (a)	Single pentagon loop diagonally cut to create two slots.....	42
Fig 3.4 (b)	RCS response of the two lengths in Fig. 23 (a)	42
Fig 3.5	Surface current distribution of the slot resonating at 28.87 GHz.....	43
Fig 3.6 (a)	The equivalent series circuit of the shortest slot	44
Fig 3.6 (b)	Reactance vs. Frequency plot for the circuit in Fig. 25 (a).....	44
Fig 3.7	Rogers RT/duroid [®] 5880 tag equipped with a Kapton [®] HN film	45
Fig 3.8	Chemical structure of a Kapton [®] HN molecule	45
Fig 3.9	Front and back view of the temperature sensing RFID tag	47

Fig 4.1	RCS response of tag designed using duroid® 5880	48
Fig 4.2	RCS response of tag designed using duroid® 5870	49
Fig 4.3	RCS response of tag designed using Taconic TLX-0	50
Fig 4.4	RCS response of tag designed using Kapton®HN with Al.....	51
Fig 4.5	RCS response of tag designed using Kapton®HN with Silver ink.....	51
Fig 4.6	RCS response of tag designed using PET with Al resonators.....	52
Fig 4.7	RCS response of tag designed using PET with Silver ink.....	53
Fig 4.8	Experimental setup for the proposed chipless RFID tag	54
Fig 4.9	Computed and measured results along H-probe.....	55
Fig 4.10	Computed and measured results along V-probe.....	55
Fig 4.11 (a)	RCS and tag design for all-ones data word	57
Fig 4.11 (b)	RCS and tag structure for all-zeros data word.....	57
Fig 4.11 (c)	RCS and tag design for 10010010100110011000100010101	57
Fig 4.12	Computed humidity sensing behavior of the proposed tag	58
Fig 4.13	Measured results of the humidity sensor	59
Fig 4.14	Temperature sensing behavior of the proposed sensor tag	60
Fig 4.15	Measured results of the temperature sensor on H-probe	61
Fig 4.16	Relationship between ϵ_r of Stanyl®TE200F6 and temperature.....	61
Fig 5.1	Total RFID market size 2021-2028.....	64
Fig 5.2	Passive RFID tag market value by type and volume in 2023.....	65

ACRONYMS

RFID	Radio Frequency Identification
IoT	Internet Of Things
IFF	Identify Friend or Foe
EM	Electromagnetic
EPC	Electronic Product Code
PET	Polyethylene Terephthalate
RF	Radio Frequency
LF	Low Frequency
HF	High Frequency
NFC	Near Field Communication
UHF	Ultra-High Frequency
BAP	Battery-assisted Power
AC	Alternating Current
RCS	Radar Cross Section
RH	Relative Humidity
CMPA	Circular Microstrip Patch Antenna
MWCNTs	Microwave Carbon Nanotubes
VNA	Vector Network Analyzer

INTRODUCTION

1.1 History of RFID

The advancement of Radio Recurrence Distinguishing proof (RFID) innovation started within the 1940s. This thought was acknowledged amid World War II when, for military purposes, radio waves were utilized for identifying hostile aircraft from friendly ones. A group driven by Watson-Watt came up with the thought of introducing transmitters in all British airplane. So, when they get a flag from the ground stations, they will rebroadcast the flag to distinguish friendly air crafts. This system is called Friend or Foe (IFF). This is how the British used radio waves to detect and locate aircraft, which laid the foundation for RFID technology [1].

In 1973, Mario W. Cardullo made significant contributions to the development of RFID technology by conceptualizing the active RFID tag. This innovative concept involved the ability to transmit information using radio waves. Cardullo's work laid the foundation for advancements in active RFID technology, enabling the transmission of data wirelessly through radio frequency (RF) signals [2]. Later in 1980s, passive tags were introduced which unlike active tags did not possess a battery and were powered by the radio waves that were emitted by the reader. It was due to these passive tags that RFID technology became more widespread. Such tags turned out to be very useful for inventory control in retail and manufacturing environment. The advancement of the Electronic Product Code (EPC) standard within the 1990s [3] cleared the way for the broad adoption of this innovation due to the interoperability between RFID frameworks. As a result, the innovation has been utilized in asset tracking, access control, and supply chain management. With the creation of a printed chip utilizing carbon nanotubes by a Korean research facility in 2010, the cost of RFID technology was further decreased [4].

In present days, RFID technology continues to evolve with advancements in antennas, chip technology, software, etc. Its use has expanded to various sectors including healthcare, aerospace, pharmaceutical industry, food and beverages industry, transportation, agriculture, logistics, etc. Moreover, its integration with sensors has allowed it to be used in a variety of devices like smartphones and other wearable technology.

1.2 Internet-of-Things (IoT) & RFID

RFID has been seamlessly integrated with other developing technology, counting the Internet-of-Things (IoT), cloud computing, and enormous information analytics. RFID is one of the empowering advances for IoT [5]. RFID technology enables the automatic identification and capture of data from RFID tags attached to objects. These tags may consist of a microchip and an antenna or just an antenna that can communicate wirelessly with RFID readers. By integrating RFID with IoT, the captured data from RFID tags can be transmitted to IoT platforms for further processing and analysis. RFID combined with IoT allows for real-time tracking and monitoring of objects. The tags can be attached to items, and with the help of RFID readers and IoT connectivity, their location and status can be continuously updated in the IoT system [6]. IoT and RFID integration enabled the creation of smart environments where objects and devices are interconnected. For example, in retail, RFID tags on products can provide information about pricing, stock availability, or expiration dates, which can be integrated with IoT systems for dynamic pricing, smart shelves, and personalized customer experiences. Similarly, in healthcare, RFID-enabled patient tracking combined with IoT can enhance patient safety, asset management, and workflow optimization. Fig. 1 illustrates some of the applications where RFID has facilitated IoT.

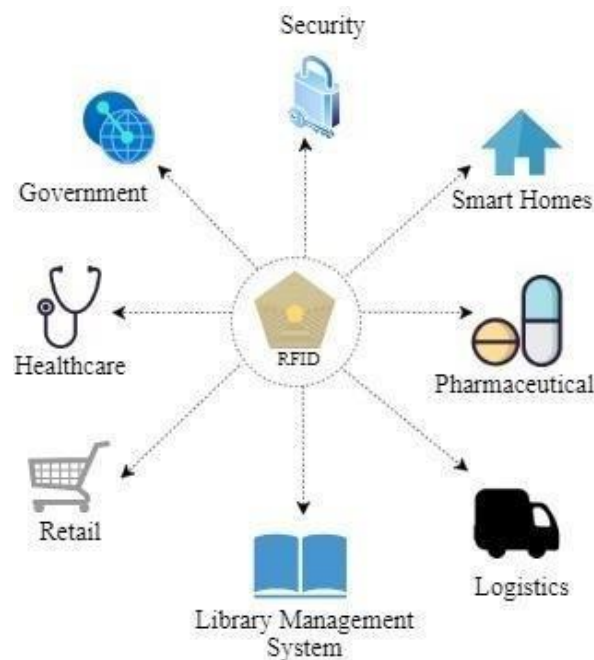


Fig. 1.1 RFID taking IoT to widespread applications.

By combining RFID with IoT, organizations gain enhanced visibility into their assets, inventory, and supply chain processes. RFID technology enables the identification and tracking of physical objects, while IoT provides the connectivity and infrastructure to gather,

analyze, and utilize the data generated by these objects. In addition, this integration enables automation, streamlines manual processes, and reduces human intervention.

1.3 Printed Electronics

Printed electronics is an emerging technology that involves the fabrication of electronic devices using printing techniques, such as inkjet printing, screen printing, or roll-to-roll printing. It offers a cost-effective and scalable approach to manufacturing electronic components and systems on flexible substrates like plastic or paper. Printed electronics enable the creation of lightweight, flexible, and even disposable electronic devices with applications across various industries [7].

One significant application of printed electronics is in the field of RFID. Printed electronics techniques allow for the mass production of RFID tags. Such printing technologies enable the deposition of conductive inks, such as silver or carbon-based inks, to create the necessary conductive tracks and components on flexible substrates [8].

The use of printed electronics in RFID brings several advantages. Firstly, it offers a cost-effective solution for large-scale production, making RFID tags more affordable and accessible for various applications. The ability to print RFID tags on flexible substrates allows for easy integration into curved or irregularly shaped objects, enhancing versatility and enabling new form factors. Additionally, printed RFID tags can be lightweight and thin, making them suitable for applications where size and weight constraints are critical. It also opens up opportunities for innovative applications. For example, printed RFID tags can be embedded in packaging, labels, or even textiles, enabling item-level tracking and inventory management. This has implications for supply chain optimization, retail, and logistics industries. Moreover, printed RFID antennas can be integrated into sensors or wearable devices, enabling the combination of RFID tracking capabilities with other functionalities, such as monitoring temperature, humidity, or vital signs.

1.4 RFID Technology

A general RFID system is a technology that utilizes radio waves for identifying and tracking objects or individuals wirelessly. It consists of three main components: RFID tags, RFID readers, and a backend system.

- 1. RFID Tags:** RFID tags encompass compact gadgets comprising a microchip as well as an antenna. These tags are classified as either active, being equipped with an internal power source like a battery, or passive, drawing energy from the RFID reader's electromagnetic field [9]. The microchip holds distinctive identification details and potentially supplementary data, while the antenna facilitates communication with RFID readers by utilizing radio waves.
- 2. RFID Readers:** RFID readers are gadgets furnished with antennas, emitting radio waves, and capturing signals from RFID tags [10]. Typically, they consist of an RF module and a controller. As an RFID tag comes into the reader's electromagnetic field, it activates and reciprocates by sending its distinct identification data to the reader.
- 3. Backend System:** The backend infrastructure takes on the task of handling and leveraging the information amassed by the RFID readers. Typically encompassing a database or software, it oversees and stores the tag-related data. Moreover, integration of the backend system with diverse systems such as inventory management, supply chain, or access control, further extends its capabilities, enabling a range of functionalities and applications.

During the manufacturing process, each RFID tag is programmed with a distinct identification number or code. It is also possible to store additional data on the tag, such as product details or maintenance history.

1.5 Types of RFID Systems

RFID technology is used for the wireless transfer of data between a tag or label and a reader device. There are several types of RFID systems, categorized based on their operating frequency and the type of tags they use. Some common types of RFID are listed below [11]:

- 1.5.1 Low-Frequency (LF) RFID:** LF RFID operates at a relatively lower frequency compared to other RFID types. The frequency range of 30 kHz to 300 kHz allows for effective communication between the reader and the tag. These tags typically have shorter read ranges compared to higher frequency RFID systems. The read range for LF RFID tags is typically a few centimeters. This limited range makes LF RFID

suitable for applications where proximity detection is required, such as access control systems or animal tracking. LF RFID systems have relatively good resistance to interference from materials such as metals and liquids. This characteristic makes them suitable for applications in environments where there are high amounts of metal or liquid present, as it reduces the impact of signal degradation. LF RFID systems generally have slower data transfer rates compared to higher frequency RFID systems. The slower data transfer is due to the lower frequency range, which limits the amount of data that can be transmitted within a given time frame. LF RFID is commonly used for applications such as access control, animal identification and tracking, and proximity-based security systems. For example, LF RFID tags are used to identify and track livestock, pets, or assets within a restricted area. LF RFID tags are designed to be compatible with LF RFID readers, ensuring seamless communication between the two components. This compatibility allows for easy integration and deployment of LFRFID systems in various environments.

1.5.2 High-Frequency (HF) RFID: HF RFID operates at a higher frequency compared to LF RFID systems. The frequency range of 3 MHz to 30 MHz enables efficient and reliable communication between the reader and the tag. HF RFID tags have moderate read ranges, typically ranging from a few centimeters to several meters. The read range can vary based on factors such as tag design, reader power, and environmental conditions. HF RFID systems offer relatively faster data transfer rates compared to LF RFID. The higher frequency range allows for quicker transmission of data between the reader and the tag, enabling faster identification and tracking processes. HF RFID technology is commonly used in applications that involve smart cards, such as contactless payment systems, electronic ticketing, and access control. HF RFID tags can be embedded in smart cards, allowing for convenient and secure transactions or access control authentication. HF RFID systems provide moderate resistance to interference from materials such as metals and liquids. While they are more susceptible to interference compared to LF RFID, proper tag and antenna placement can minimize the impact of interference and optimize read performance. HF RFID technology finds widespread use in various industries and applications. It is commonly utilized for applications such as access control systems, inventory management, library book tracking, supply chain management, and product authentication.

1.5.3 Near Field Communication (NFC): NFC is a subset of HF RFID that operates at 13.56 MHz. NFC is primarily used for short-range communication, typically within a few centimeters. It is designed to be compatible with existing HF RFID standards, enabling NFC-enabled devices to interact with other NFC devices or HF RFID tags. This compatibility allows for seamless integration and interoperability between different NFC-enabled devices. It is commonly found in applications like contactless payment systems, mobile device communication, and smart home devices.

1.5.4 Ultra-High Frequency (UHF) RFID: UHF RFID operates at a higher frequency compared to LF and HF RFID systems. The frequency range of 300 MHz to 3 GHz allows for longer-range communication between the reader and the tag. UHF RFID tags offer long read ranges, typically ranging from several meters to tens of meters. The extended read range makes UHF RFID suitable for applications where items need to be identified and tracked over greater distances, such as supply chain management and logistics. UHF RFID systems provide faster data transfer rates compared to LF and HF RFID. The higher frequency range enables rapid transmission of data between the reader and the tag, facilitating efficient inventory management and tracking processes. UHF RFID systems can be more susceptible to interference from materials such as metals and liquids compared to LF and HF RFID. Interference can affect the read performance and reliability of the system. Proper tag and antenna placement, as well as frequency hopping techniques, can mitigate interference issues. UHF RFID systems operate in a wideband spectrum, which allows for increased tag capacity and the ability to support multiple tags simultaneously. This feature is advantageous for scenarios that involve bulk reading of multiple RFID tags, such as retail inventory management or asset tracking. UHF RFID technology finds widespread use in various industries and applications. It is commonly used for applications such as supply chain management, inventory tracking, retail tracking, vehicle identification, and asset management.

1.6 Classification of RFID Tags

RFID tags can be classified based on various factors, including their power source, form factor, memory capacity, and read/write capabilities. Here is a breakdown of the classification of RFID tags:

1.6.1 Active RFID Tags: Active RFID tags are a type of RFID tag that have their own power source, typically a battery [12]. Unlike passive RFID tags that rely on energy from the RFID reader's electromagnetic field, active tags actively transmit signals to the reader, allowing for longer read ranges and real-time tracking capabilities. Active RFID tags are equipped with an internal power source, usually a battery. A commercial active RFID tag has been shown in Fig. 2.



Fig. 1.2 A commercial active RFID Tag (Courtesy: <https://www.infinidtech.com/v-tag-gps-products>)

The battery powers the tag's circuitry and enables it to actively transmit signals. The power source provides continuous energy to the tag, allowing it to operate independently of the RFID reader. Active RFID tags have significantly longer read ranges compared to passive tags. The read range can range from tens of meters to hundreds of meters, depending on the specific tag and reader configuration. The extended read range makes active tags suitable for applications that require tracking or monitoring objects over larger distances. Active tags enable real-time tracking of assets or objects. As they continuously transmit signals, they provide up-to-date information about the tag's location and status. Real-time tracking is particularly useful in applications such as supply chain management, vehicle tracking, and inventory management, where timely and accurate information is critical. Active RFID tags generally have a larger memory capacity compared to passive tags. This allows them to store more data, such as sensor readings, environmental conditions, or historical information. The increased data storage capacity enables active tags to capture and store additional information related to the tracked assets or objects. Active RFID tags are typically larger in size and more expensive compared to passive tags. The inclusion of a battery and additional circuitry contributes to the larger form factor

and higher cost. However, advancements in technology have resulted in smaller and more cost-effective active tags over time. Active RFID tags find application in various industries and use cases. They are commonly used for asset tracking, container tracking, inventory management, fleet management, and personnel tracking. For instance, in logistics, active tags can provide real-time location updates of shipments, ensuring better visibility and security throughout the supply chain.

1.6.2 Passive RFID Tags: Passive RFID tags are a type of RFID tag that does not have an internal power source [13]. Instead, they rely on the energy harvested from the RFID reader's electromagnetic field to power the tag's circuitry and enable communication with the reader. Passive RFID tags do not have their own power source, such as a battery. An example is shown in Fig. 3.



Fig. 1.3 A passive RFID tag (Courtesy: Radio Frequency Identification: <https://telecom.altanai.com/tag/passive-rfid-tags/>)

They draw power from the electromagnetic field generated by the RFID reader during communication. The energy harvested from the reader's field is used to power the tag's circuitry, allowing it to respond to the reader's queries. Passive RFID tags have shorter read ranges compared to active RFID tags. The read range can vary depending on factors such as the frequency used, tag design, reader power, and environmental conditions. In general, read ranges for passive tags can range from a few centimeters to several meters. Passive tags rely on backscatter` technology to communicate with the reader. When the reader's electromagnetic field energizes the tag, the tag modulates or reflects the field back to the reader. This modulation contains the tag's unique identifier (ID) and any additional data stored on the tag. Passive RFID tags are typically smaller and less expensive compared to active tags. Their

simpler design, lack of battery, and reduced components contribute to their smaller form factor and lower cost. This makes passive tags more suitable for applications where cost and size constraints are important factors. Passive RFID tags have a wide range of applications across various industries. They are commonly used in inventory management, supply chain tracking, access control, asset tracking, and retail inventory management. For example, in retail, passive tags can be attached to individual items to track inventory levels, reduce theft, and improve overall supply chain efficiency.

1.6.3 Semi-Passive RFID Tags: Semi-passive RFID tags, also known as battery-assisted passive (BAP) tags, are a type of RFID tag that combines characteristics of both active and passive tags [14]. Semi-passive tags have a small onboard battery that powers specific functionalities of the tag, while still relying on the energy from the RFID reader for communication. Semi-passive RFID tags contain a small onboard battery that powers certain features of the tag, such as onboard sensors, data storage, or additional circuitry. One such semi-passive RFID tag has been shown in Fig. 4.

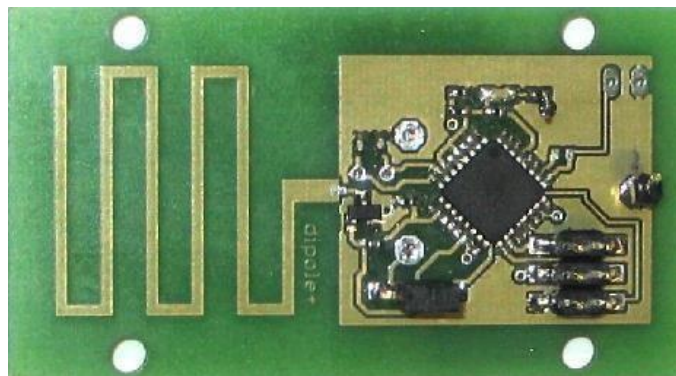


Fig. 1.4 A semi-passive RFID Tag [14]

The battery provides the necessary energy to support these functionalities while the tag still relies on the RFID reader's electromagnetic field for communication power. Like passive RFID tags, the read range of semi-passive tags depends on factors such as frequency, tag design, and reader power. It typically ranges from a few centimeters to several meters, depending on the specific configuration. The BAP allows for improved read ranges compared to purely passive tags. Semi-passive tags employ similar backscatter technology as passive tags for communication with the

RFID reader. When energized by the reader's electromagnetic field, the tag reflects or modulates the field back to the reader, allowing for data transmission. The onboard battery in semi-passive tags powers additional functionalities. These features can include sensors for temperature, humidity, or motion detection, which allow the tag to collect and transmit environmental data. The battery may also support increased data storage capacity, enabling the tag to store and transmit more information. The battery assistance in semi-passive tags provides increased sensitivity and responsiveness compared to pure passive tags. This enhanced readability can result in improved read rates and reliability, especially in challenging environments with weak or noisy reader signals. Semi-passive RFID tags are typically larger and more expensive than passive tags due to the inclusion of the onboard battery and additional components. However, advancements in technology have allowed for smaller and more cost-effective semi-passive tag designs over time.

1.7 Coupling Mechanisms

RFID technology utilizes different coupling mechanisms to establish communication between RFID tags and readers. These coupling mechanisms enable the transfer of data and power between the two components. There are four coupling mechanisms between the RFID tag (transponder) and the reader, which vary based on the type of tag (passive, active, or semi-active) [15].

1.7.1 Inductive Coupling: Inductive coupling, also known as near field coupling or magnetic coupling, is widely utilized in LF and HF RFID systems. It involves the interaction between the magnetic fields generated by the reader and the tag to establish communication. In this coupling mechanism, the RFID reader generates an alternating current (AC) through its transmitter coil antenna. The alternating current flowing through the coil creates an alternating magnetic field around it. The RFID tag, equipped with a receiver coil antenna, is placed near the reader's magnetic field. The magnetic field generated by the reader's coil induces a voltage in the receiver coil of the tag through electromagnetic induction. This induced voltage powers the tag's circuitry and enables data transmission. The tag modulates the magnetic field by altering the load or impedance on its coil antenna. This modulation encodes information such as the tag's identification data or additional data stored on the tag. The reader's coil detects the changes in the magnetic field caused by the modulation

and decodes the information transmitted by the tag. This enables data retrieval and identification of the tag. The process is shown in Fig. 5.

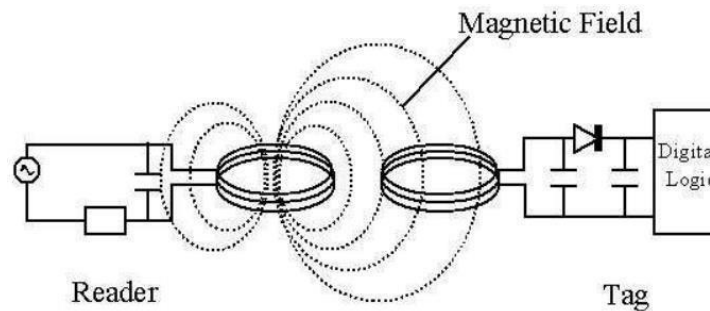


Fig. 1.5 An RFID system with inductive coupling

Inductive coupling allows for short-range communication between the reader and the tag, typically within a few centimeters to a few meters. The range depends on factors such as the power of the reader's transmitter, the design of the antennas, and environmental conditions. Inductive coupling is advantageous in environments where close-range detection and reliable communication are required. It is less susceptible to interference from metals and liquids compared to other coupling mechanisms, making it suitable for applications such as access control, asset tracking, and proximity-based systems.

1.7.2 Backscatter Coupling: Backscatter coupling, also known as backscatter modulation or backscattering, is commonly used in passive RFID systems, particularly in UHF RFID. It allows for wireless communication and data exchange between the reader and the tag. In this coupling mechanism, the RFID reader emits a continuous or modulated RF signal. When the RF signal reaches the RFID tag, it is incident upon the tag's antenna. Instead of directly absorbing the energy, the tag reflects or backscatters the signal back towards the reader. The backscattered signal carries information encoded by the tag, such as its unique identifier or additional data. The modulation or alteration of the reflected signal is achieved by modifying the tag's impedance or load in response to the incoming RF signal. The RFID reader detects and decodes the modulated backscattered signal, allowing for data retrieval and identification of the tag. The reader can extract the transmitted information and process it as required for various applications, such as inventory management or access control. A general backscatter coupling RFID system is shown in Fig. 6.

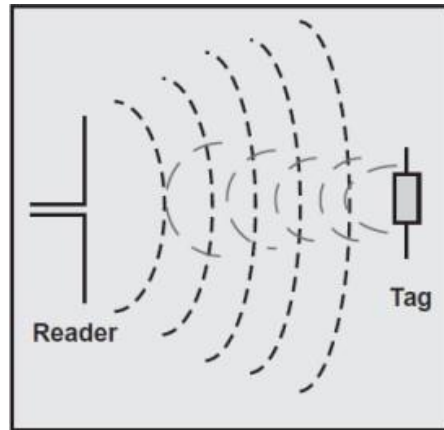


Fig. 1.6 An RFID system with backscatter coupling

Backscatter coupling offers several advantages in RFID systems. It enables long-range communication between the reader and the tag, typically ranging from a few meters to tens of meters. The long read range facilitates efficient data collection and identification of multiple tags simultaneously, improving overall system performance. Backscatter coupling allows for passive RFID tags that do not require a power source, resulting in smaller tag size and longer operational lifespan. The lack of an internal power source makes passive backscatter tags cost-effective and easy to deploy in large-scale applications. However, backscatter coupling is susceptible to interference and environmental factors that can affect the quality of communication. Factors such as metallic objects, liquid substances, and electromagnetic noise can impact the signal integrity and read performance.

1.7.3 Transmitter Type: Transmitter type coupling, also known as far field coupling or electromagnetic coupling, is commonly used in RFID systems operating at higher frequencies, such as UHF and microwave frequencies. It involves the transmission of radio waves from the reader's transmitter antenna to the tag's receiver antenna. In this coupling mechanism, the RFID reader emits a continuous wave or modulated signal at the designated frequency. The transmitter antenna generates an electromagnetic field, which propagates through the air or other media. The tag's receiver antenna, tuned to the same frequency, intercepts the transmitted signal. The receiver antenna captures the electromagnetic energy from the transmitted signal. The energy is then rectified and utilized to power the tag's circuitry. This energy harvesting process enables the passive tag to activate and respond to the reader's query or commands. Transmitter

type coupling allows for longer communication distances between the reader and the tag compared to near field coupling mechanisms. It enables read ranges ranging from a few meters to tens of meters or more, depending on the specific RFID system configuration and environmental factors.

1.7.4 Transponder Type: Transponder type coupling, also known as near field coupling or inductive coupling, is commonly used in RFID systems operating at lower frequencies, such as LF and HF. It involves the proximity of the reader and the transponder for communication. In this coupling mechanism, the RFID reader generates an alternating magnetic field using its transmitter antenna. The magnetic field induces a voltage in the receiver antenna of the transponder. The transponder uses this induced voltage to power its circuitry and respond to the reader's queries. The transponder, which may be passive or semi-passive, modulates the backscattered signal or changes the load on its receiver antenna to encode data. The reader detects these changes in the magnetic field and decodes the information transmitted by the transponder. Transponder type coupling allows for relatively short communication distances between the reader and the transponder, typically within a few centimeters to a few meters. This proximity-based coupling enables reliable and efficient communication, making it suitable for applications such as access control, asset tracking, and proximity-based systems.

1.8 Applications of RFID Technology

RFID technology finds diverse applications across various fields, offering advantages such as automation, improved efficiency, and enhanced tracking capabilities. Let's explore some notable applications of RFID technology in different industries [16]:

1.8.1 Retail: RFID technology revolutionizes inventory management by enabling real-time tracking and automated stock control. RFID tags attached to products provide accurate information on inventory levels, allowing retailers to optimize replenishment, reduce out-of-stock situations, and improve overall supply chain efficiency. RFID-based systems also help combat theft and counterfeiting through enhanced product authentication.

- 1.8.2 Logistics and Supply Chain Management:** RFID technology plays a crucial role in streamlining logistics and supply chain operations. It enables real-time tracking and tracing of goods, improving visibility, and reducing errors in inventory management. RFID tags on packages, pallets, or containers facilitate automated data capture, ensuring accurate shipment verification, reducing manual handling, and enhancing overall logistics efficiency.
- 1.8.3 Healthcare:** RFID technology enhances patient safety, inventory management, and asset tracking in healthcare settings. RFID tags embedded in patient wristbands can help accurately identify patients, track their movements, and ensure correct medication administration. RFID systems also facilitate inventory management of medical supplies, reduce manual efforts in tracking medical equipment, and enable efficient asset utilization in hospitals.
- 1.8.4 Manufacturing:** RFID technology is used in manufacturing processes for asset tracking, work-in-progress monitoring, and quality control. RFID tags attached to components or products enable accurate tracking throughout the production cycle, enabling better inventory control, reducing errors, and improving process efficiency. RFID-based systems also support traceability and recall management by providing quick access to product information and history.
- 1.8.5 Automotive Industry:** RFID technology is utilized for vehicle tracking, anti-theft systems, and supply chain management in the automotive industry. RFID tags embedded in vehicles or components enable accurate tracking during production, logistics, and distribution processes. This enhances efficiency in assembly lines, optimizes inventory control, and improves overall supply chain visibility and security.
- 1.8.6 Hospitality and Events:** RFID wristbands or cards are widely used in the hospitality and events industry for access control, cashless payments, and personalized experiences. RFID technology enables seamless entry to venues, contactless transactions at concessions, and targeted marketing based on attendee behavior. It enhances security, reduces waiting times, and offers a convenient and enjoyable experience for guests.

1.8.7 Agriculture and Livestock: RFID technology is utilized for animal identification, tracking, and monitoring in agriculture and livestock management. RFID ear tags or implants help in individual animal identification, disease control, breeding management, and tracking livestock movements. This technology aids in improving traceability, ensuring food safety, and optimizing livestock operations.

These are just a few examples of how RFID technology is applied across different industries. Its versatility, coupled with advancements in tag design and reader technology, continues to drive innovation and find new applications. With the ability to enhance efficiency, accuracy, and automation, RFID technology plays a significant role in transforming processes and operations across diverse fields.

1.9 Sensor Integration

The utilization of discrete environmental sensors for large-scale deployment is not economically viable due to their high cost. Nevertheless, a practical and cost-effective alternative arises through the integration of chipless RFID tags with sensors, offering immense potential for widespread sensing applications. These innovative sensing tags are engineered using substrates that exhibit alterations in their electrical properties in response to changes in specific environmental parameters [17]. By incorporating these modified substrates into the design of chipless RFID tags, the tags gain the ability to act as sensors, detecting and recording variations in environmental conditions. This transformative approach allows for the creation of versatile and affordable sensing solutions, facilitating extensive deployment across various industries and applications. The cost-effectiveness and adaptability of these integrated chipless RFID tags with sensors open up new possibilities for harnessing the power of IoT and advancing the concept of a connected world.

1.10 Objectives

The objectives of this research work are listed as follows:

- a. To develop a cost-effective and compact chipless RFID tag with a unique design that enables the tagging of multiple items simultaneously.

- b. To implement chipless RFID technology on different substrates to enable the use of the tag in diverse environmental conditions.
- c. To utilize a substrate that provides both sensitivity and item tagging capabilities.
- d. To enable the printable functionality of the tag to facilitate mass production.
- e. To ensure the flexibility of the tag to enable its use on irregular surfaces.
- f. To maximize band utilization efficiency to achieve multiple bits with a reduced frequency band.

1.11 Organization of the Thesis

The thesis begins with Chapter 1, which provides an extensive introduction to RFID tags, encompassing their working principles, wide-ranging applications, various types of RFID systems, and their integration with IoT. Chapter 2 delves into a comprehensive literature review, analyzing and comparing the proposed RFID tag with previously published tags. Chapter 3 focuses on the architecture of the proposed RFID tag, elucidating the design principles. Chapter 4 presents the results and discussion, highlighting the outcomes of experiments conducted to evaluate the proposed RFID tag's performance. It analyzes the tag performance using various substrates. Chapter 5 concludes the thesis by summarizing the achievements, reiterating the significance of the research contributions, and outlining potential future research directions. Finally, the thesis ends with a bibliography, citing the relevant sources used throughout the research process.

LITERATURE REVIEW

A lot of different approaches, techniques, and advancements that have been proposed and implemented in the design and operation of chipless RFID tags. A wide range of scholarly articles, conference papers, patents, and technical reports to establish a comprehensive understanding of the current state of chipless RFID technology are present in the literature. This chapter aims to explore and evaluate the existing research and developments in the field of chipless RFID tags.

[18] introduces a chipless RFID tag having a coding capacity of 11 bits. The resonator design proposed in this study consists of truncated elliptical shapes formed by non-continuous arc slots. The slots exhibit a 1:1 correspondence between slots and bits as shown in Fig. 7(b). The electromagnetic performance of the tag design is analyzed using an ungrounded Rogers RT duroid® 5880 laminate. The overall size of the tag is shown in Fig. 7

(a) which is $15 \times 15 \times 0.508 \text{ mm}^3$, resulting in a bit density of 4.88 bits/cm^2 .

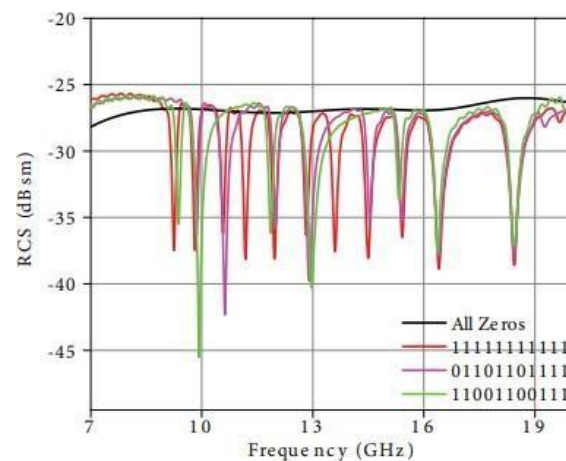
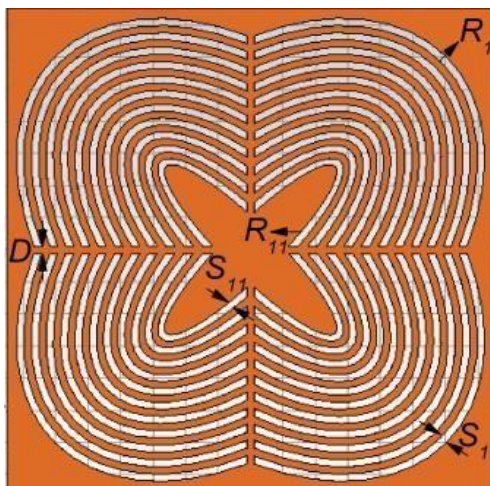


Fig. 2.1 (a) Design of the tag presented in [18] (b) RCS response of the same tag.

A chipless RFID system is introduced in [19]. As illustrated in Fig. 8 (b), the tag exhibits the ability to encode 12-bit data within the 3 to 6 GHz frequency range. This system consists of a completely printable chipless tag and a set of reader antennas with high gain. The process of information encoding into the frequency spectrum is accomplished by employing a multi-

resonant circuit. This circuit is constructed using a distinctive arrangement of various microstrip resonators, including U and L-shaped open stub resonators, as depicted in Fig. 8 (a).

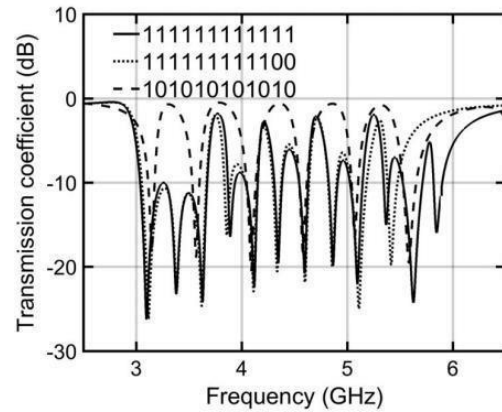
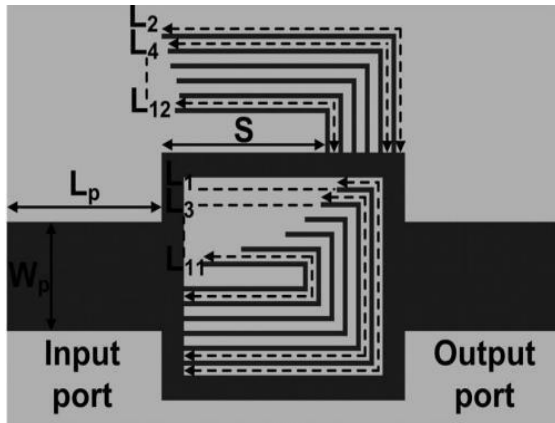


Fig. 2.2 (a) Design of the RFID tag in [19]

(b) Frequency response of the tag in [19]

In reference [20], a chipless RFID tag is introduced, showcasing both an impressive data capacity of 22 bits and a versatile sensing ability for multiple parameters. The tag, which boasts a radius of 7.4 mm, interacts with incident plane waves that are dual-polarized. It employs a substrate based on Kapton[®] HN, integrated with copper as the radiating material. Additionally, the tag employs multiwall carbon nanotubes (MWCNTs) to function as a CO₂ sensor. This tag's frequency response is observable across the frequency range of 4 to 25 GHz. The structure of the tag, along with its radar cross-section (RCS) response, can be observed in Fig. 9 (a) and 9 (b), respectively.

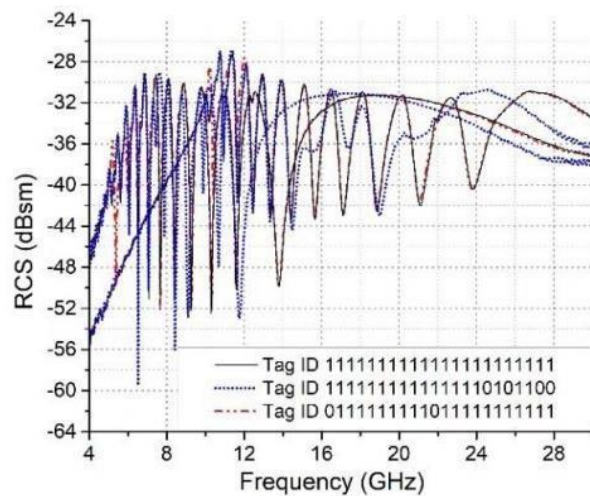
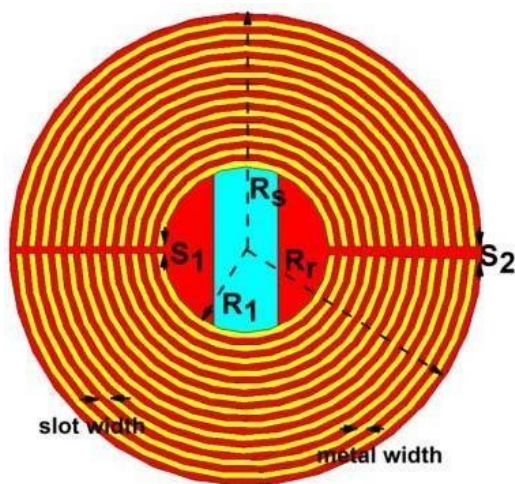


Fig. 2.3 (a) Layout of the tag in [20]

(b) RCS response of the tag in [20]

In [21], a passive RFID tag is introduced, characterized by its compact size and insensitivity to polarization. The tag's design centers around slotted elliptical structures that are ingeniously arranged in a nested loop pattern, with the slot resonators having uniform dimensions, as illustrated in Fig. 10 (a). This RFID tag boasts a data storage capability of 10 bits and functions across a spectral range spanning from 3.6 to 15.6 GHz, as depicted in Fig. 10 (b). The proposed tag architecture undergoes thorough analysis and refinement for different substrates—specifically, Rogers RT/duroid/5880, Rogers RT/duroid/5870, and Taconic TLX-0—while being confined within a compact footprint of 22.8 x 16 mm².

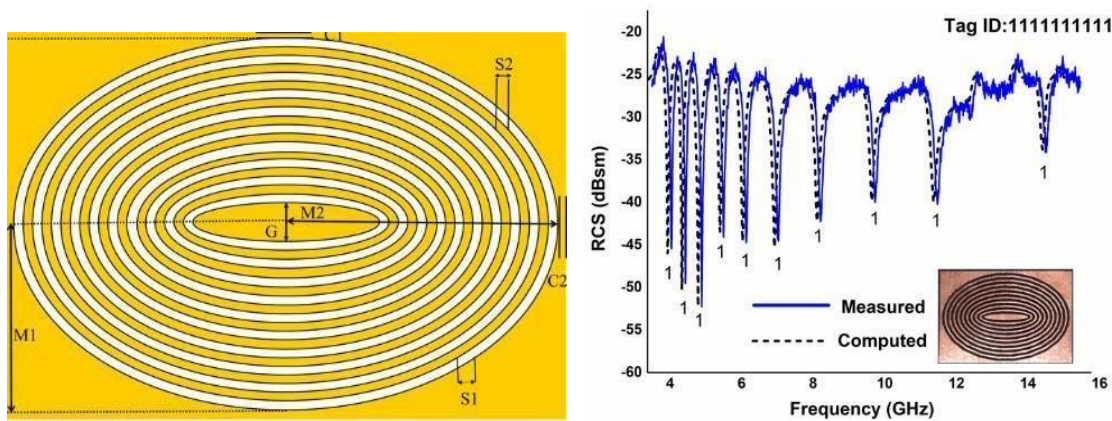


Fig. 2.4 (a) Structure of the tag in [21]

(b) RCS response of the tag in [21]

The study in [22] delved into the behavior of a moving chipless RFID tag as it moved to different discrete positions in the XY-coordinates. This tag employed slot resonators shaped like the symbol 'Δ', as visualized in Fig. 11 (a). The RFID tag, measuring 25.71 cm² in size, was modeled, utilizing Taconic TLX-8 as the substrate material. The chosen substrate had a permittivity value of 2.55, a thickness of 0.13, and a loss tangent of 0.0019. The simulation outcomes for the tag's response are presented in Fig. 11 (b).

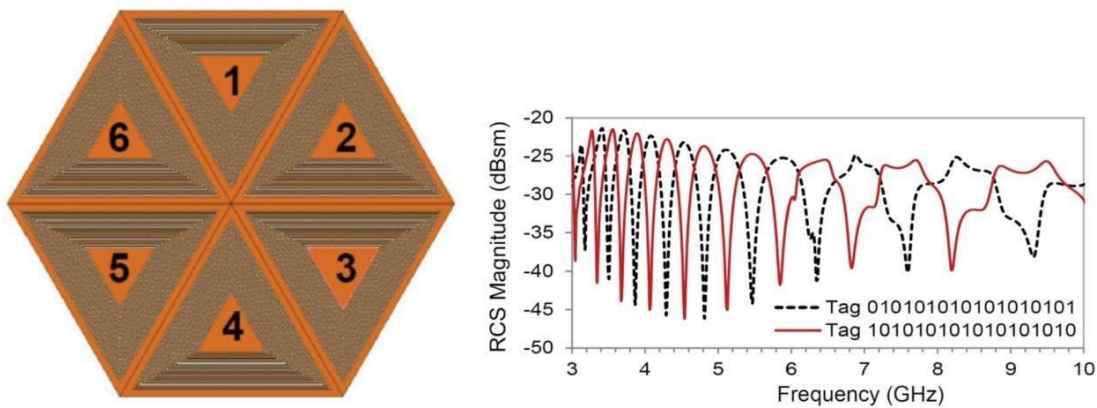


Fig. 2.5 (a) Design of the tag in [22]

(b) RCS response of the tag in [22]

In [23], a fully passive chipless RFID tag with dimensions of $16 \times 15 \text{ mm}^2$ is introduced. This tag offers a substantial data storage capacity of 15 bits and employs the ON-OFF keying principle to encode data within its compact structure. The resonating structure of the tag adopts a loop-based pentagonal geometry, depicted in Fig. 12 (a). Remarkably, this chipless RFID tag attains a noteworthy bit density of 6.25 bits/cm^2 and functions within a frequency range spanning from 4.8 to 18.8 GHz, as showcased in Fig. 12 (b). To evaluate the electromagnetic performance of the tag's design, investigations are conducted using ungrounded laminates, specifically Rogers RT/duroid[®] 5880 and Rogers RT/duroid[®] 5870.

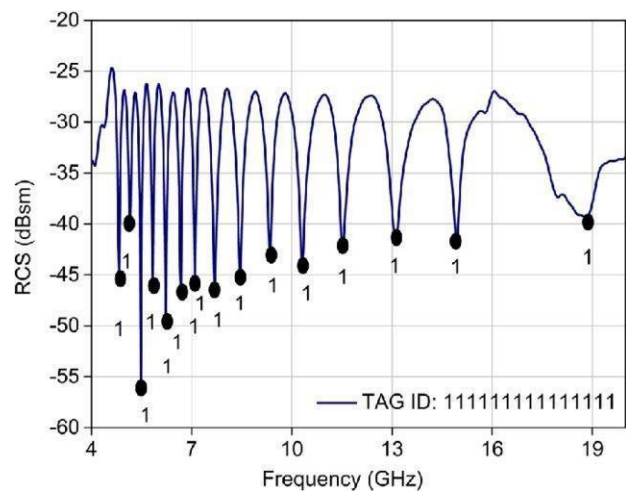
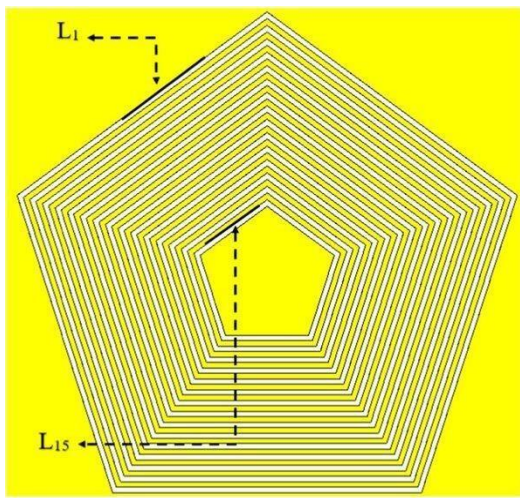


Fig. 2.6 (a) Geometry of the tag in [23]

(b) RCS response of the same pentagonal tag

The study documented in [24] presents an innovative chipless RFID tag employing a nested octagon structure that is impervious to polarization. This tag possesses an encoding capacity of 12 bits and exhibits a direct correspondence of 1:1 between its slots and bits. Crafted with precision, the tag maintains a compact size, measuring $23 \times 23 \text{ mm}^2$, ultimately yielding a remarkable bit density of 2.26 bits/cm^2 . The fabrication of this tag is executed using the flexible Rogers RT/duroid[®] 5880 laminate. The tag's distinctive geometry and its electromagnetic response are meticulously detailed in Fig. 13 (a) and (b) respectively.

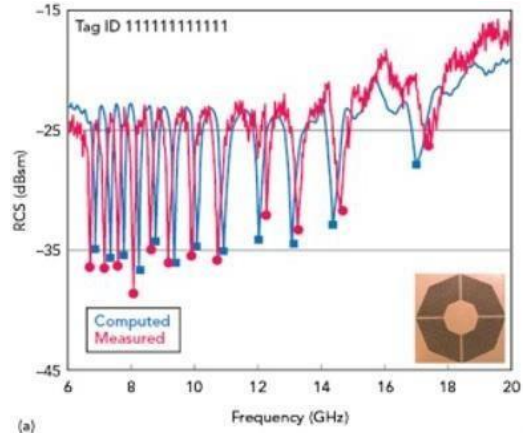
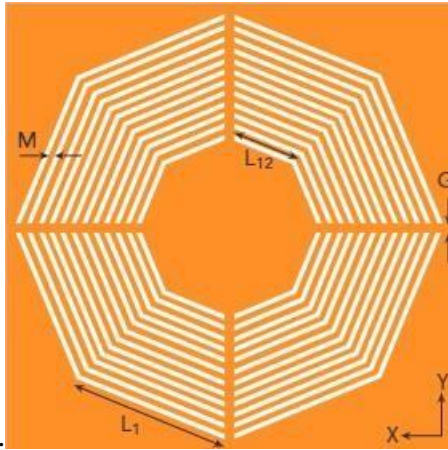


Fig. 2.7 (a) Geometry of the tag in [24] (b) RCS response of the octagonal tag in [24]

The study detailed in [25] introduces 7-bit chipless RFID multi-parameter sensor. This sensor is ingeniously devised using the advanced Rogers RT/Duroid 6010.2LM material. The sensor's architecture comprises six resonators in inverted U and L shapes, meticulously crafted with specific dimensions to resonate within the targeted frequency spectrum of 2-8 GHz. To facilitate the characterization of cracks, a circular microstrip patch antenna (CMPA) is incorporated. The developed sensor possesses the capability to monitor cracks in metal surfaces, a context where temperature monitoring is of paramount importance. The design of the sensor, alongside its RCS response, is vividly depicted in Fig. 14 (a) and (b) respectively.

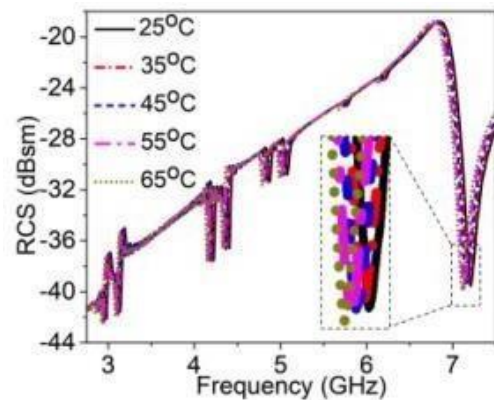
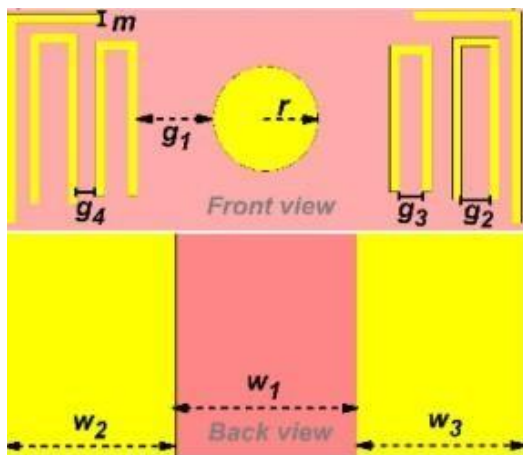


Fig. 2.8 (a) Layout of the tag in [25] (b) Corresponding RCS response of the tag

The research presented in [26] introduces a chipless RFID tag spanning 11 bits and displaying polarization-independent attributes. This tag encompasses a frequency-selective surface, effectively catering to encoding purposes as well as RH sensing applications. The

architecture employs ten exterior U-shaped resonators for item encoding, while the interior resonator employs Kapton[®] material for RH sensing. Operating within the S- and C- frequency bands, this RFID tag exhibits a noteworthy fractional bandwidth of up to 88%, culminating in an impressive density of 4.46 bits/cm². The study undertakes an investigation into both single- and dual-layer tags, delving into their respective characteristics. The structure of the tag, along with its corresponding RCS response, is thoughtfully depicted in Fig. 15 (a) and (b) respectively.

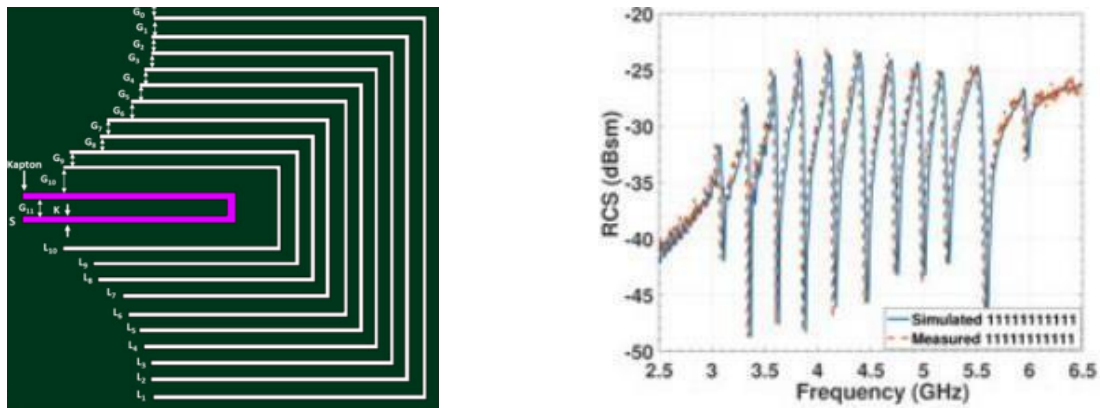


Fig. 2.9 (a) Geometry of the tag in [26] (b) corresponding RCS response of the same tag

The chipless RFID tag in [27] is a 22-bit passive tag illustrated in Fig. 16 (a). The tag design incorporates 'U' and 'Inverted-U' shaped slots etched on a metallic plate measuring 39x40 mm², enabling a data capacity of 22 bits and the potential to label 4,194,304 objects. The optimization process focuses on Taconic TLX-0 and RT/duroid[®]5880 substrates. The corresponding RCS response for both the substrates is shown in Fig. 16 (b).

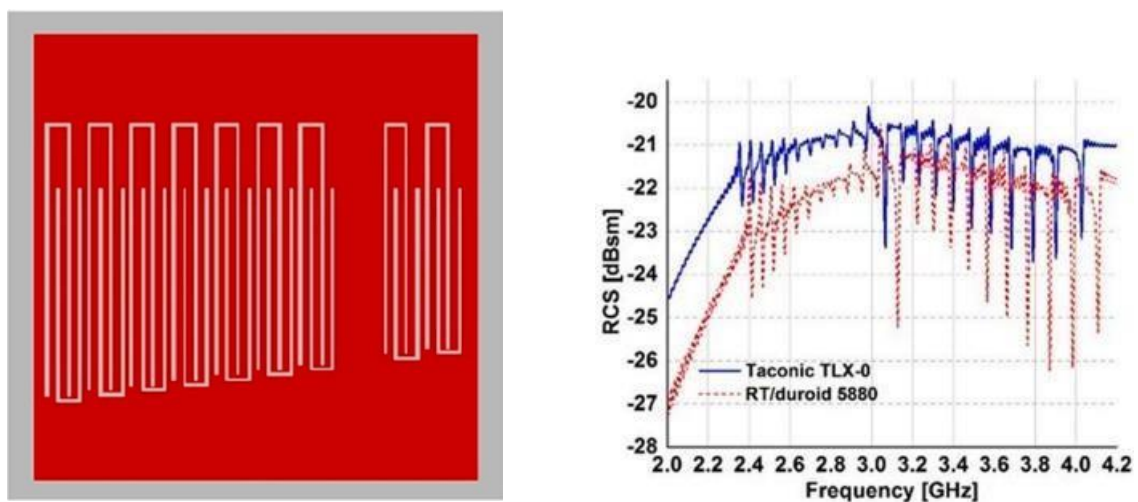


Fig. 2.10 (a) Layout of the tag in [27] (b) RCS response of the tag in [27]

The tag in [28] is designed on a PET substrate, featuring a size of 1 cm radius and operating in the ultra-wideband frequency range of 3.5 to 16 GHz. The suggested sensor tag exhibits a high code density of 6.92 bits/cm², a regular geometry, increased sensitivity to humidity variations of 60% RH, high magnitude frequency dips, and angular stability up to 60°. Fig. 17 (a) and (b) show structure and RCS response of the given tag.

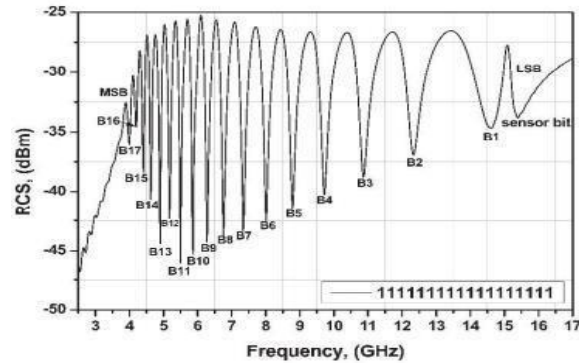
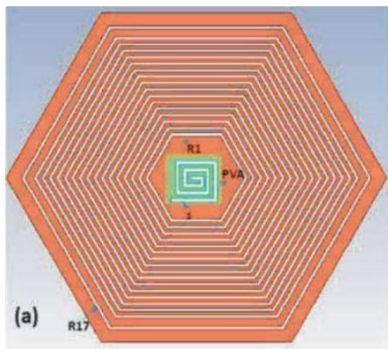


Fig. 2.11 (a) Design of the tag in [28]

(b) RCS response of the tag in [28]

The study in [29] presents a frequency-coded chipless RFID tag designed for the Ku-band frequency range (12.4-18 GHz). To assess the performance of the chipless RFID tag, four 3-bit tags are designed and simulated, with two of them manufactured and tested. The simulations and measurements focus on codes 000 and 111, confirming the effectiveness of the proposed design. Additionally, the paper explores the tag's sensitivity to fabrication errors and orientation, providing simulations that demonstrate these aspects.

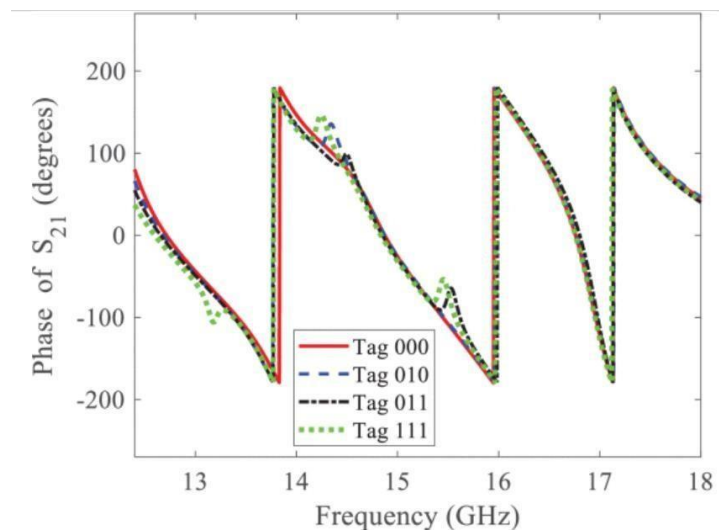
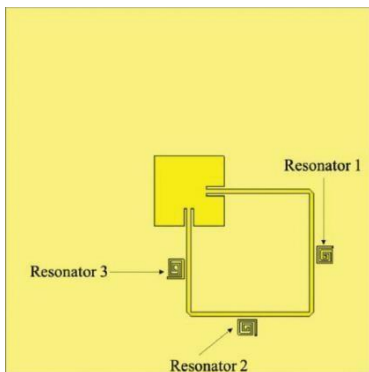


Fig. 2.12 (a) Structure of the tag in [29]

(b) RCS response of the same tag.

The study presented in [30] introduces an innovative printable Chipless RFID tag boasting a 30-bit capacity and enhanced read range capabilities. The tag's structure is composed of two distinct triangular patches meticulously arranged in a fan-like configuration, as demonstrated in Fig. 19 (a). This unique arrangement contributes to the tag's improved read range performance. The proposed tag design undergoes comprehensive analysis utilizing a range of substrates, which include Taconic (TLX-8), Rogers RT/Duroid[®] (5880), PET, and Kapton[®] HN. This diversity in substrate options grants the tag adaptability to various environmental conditions. The optimization process takes place on Dupont Kapton[®] HN substrate, utilizing silver nanoparticle ink as the radiator material. The resultant tag, measuring $55.3 \times 55.3 \text{ mm}^2$, operates within a frequency band spanning from 2.63 to 9.22 GHz, as illustrated in Fig. 19 (b).

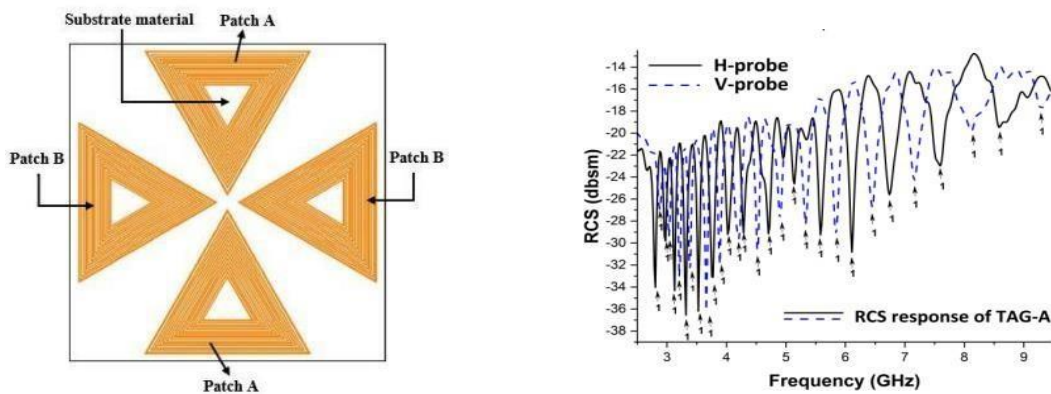


Fig. 2.13 (a) Tag Configuration in [30]

(b) RCS response of the tag in [30]

PROPOSED CHIPLESS RFID TAG

This research introduces a novel data-dense, miniaturized, and fully printable multi-sensor RFID tag, specifically designed for data encoding and sensing purposes. The tag's development involves a flexible substrate called Rogers RT/duroid[®]5880, with copper resonators sized at 15 x 16 mm². Further evaluation was conducted on PET and Kapton[®]HN substrates, both of which are flexible. The unique slot-resonator geometry of the tag enables the encoding of 29 bits, corresponding to 29 slots within the tag structure. The tag itself has a pentagonal shape, partitioned into 14 H-polarized slots and 15 V-polarized slots through metal radiators. One of the distinctive features of this research is the inclusion of a built-in multi-sensing capability, achieved by incorporating a humidity-sensitive substrate, Kapton[®]HN, and a temperature-dependent polymer, Stanyl[®] polyamide. This novel combination enables the tag to perform multiple sensing functions effectively.

This research stands out due to its compact design, ease of fabrication, high data encoding capacity, and its ability to identify 2²⁹ unique items, making it a significant advancement in the field of RFID technology and data sensing applications.

3.1 Fundamental Operation of the Tag

The chipless RFID tag operates on the backscattering technique, eliminating the need for external circuitry or power source to activate the tag. To retrieve data from the tag, the reader transmits an RF wave towards it; equation (1) representing the instantaneous E-field of the incident plane wave.

$$E(z;t) = a_x Re[E_{x0} e^{j(\omega t + kz + \varphi x)}] + a_y Re[E_{y0} e^{j(\omega t + kz + \varphi y)}] \quad (1)$$

After EM signal is transmitted to the tag [31], the tag draws power from this incident signal. The Friis transmission equation (2) calculates the power extracted by the tag, taking into account factors such as distance (r) between the transmitter and receiver, the transmitted power (P_{TX}), and the gains of transmitting (G_{TX}) and receiving (G_{RX}) antennas [32].

$$\frac{P_{RX}}{P_{TX}} = \left(\frac{\lambda}{4\pi r}\right)^2 G_{TX} G_{RX} \quad (2)$$

Upon receiving the signal, the tag responds uniquely and scatters the encoded information back to the reader. This information is decoded and subsequently stored in the host computer. Chipless RFID tags store data in their structure, which can include resonators, microstrip lines, antennas, and other elements. The process is illustrated in Fig. 20.

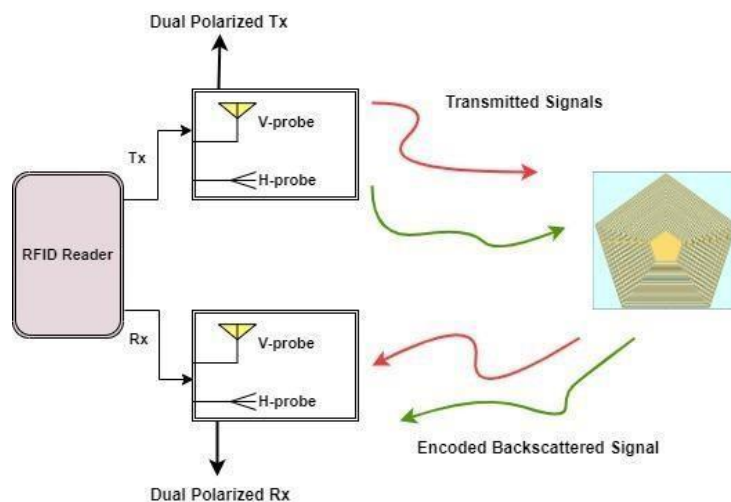


Fig. 3.1 Backscattering phenomena in chipless RFID tags

The RCS response, responsible for providing the unique frequency signature of the tag, plays a crucial role in object identification through its electromagnetic behavior. To measure RCS, the tag needs to be positioned at a distance determined by the Fraunhofer distance formula [33]. The formula for the Fraunhofer distance (R) is given in equation (3):

$$R = \frac{2D^2}{\lambda} \quad (3)$$

Here, D represents the greatest dimension of the tag, and λ symbolizes the wavelength of the radio waves. For the proposed tag, the calculated far-field distance is 40 mm.

For an item to be successfully identified, it must fall within the read range of the RFID system. The read range is defined as the maximum theoretical distance between the reader and the remotely located tag, and it is expressed in equation (4). This distance represents the range within which a chipless RFID tag can be activated by the reader without requiring any additional power for its operation [34].

$$R_{\max} = \frac{4}{\sqrt{(4\pi^3)P_r}} \frac{G_r P_t G_t \lambda^2 \sigma}{\quad} \quad (4)$$

In the given equation, the variables G_r and G_t represent the gains of the receiving and transmitting antennas, respectively. P_t stands for the power of the transmitter, while P_r

symbolizes the sensitivity of the receiver. λ denotes the wavelength, and σ represents the RCS response of the tag.

3.2 Development of the Proposed Tag

The design and optimization of the proposed tag are carried out using CST Microwave Studio Suite[®]. The tag is fabricated on an ungrounded, flexible laminate known as Rogers RT/duroid[®] 5880. To evaluate its performance, the tag is illuminated with both horizontally and vertically polarized plane waves directed towards its surface. To enhance the data density of the tag and achieve 29 slots corresponding to 29 unique frequencies in the RCS response, the slots are separated by metal radiators as shown in Fig. 22. Each frequency dip in the tag's response represents a logic state of '1', while the absence of a dip indicates a logic state of '0'. This approach effectively encodes information and increases the tag's capacity to carry data. Fig. 19 displays the arrangement of the tag in the simulation setup. In order to capture and analyze the backscattered signal, both the E-field (far-field) and RCS probes are accurately positioned at a distance of 40 mm within the far-field region. The tag, which is dual-polarized, consists of 14 horizontally polarized slots and 15 vertically polarized slots, necessitating the use of a linearly dual-polarized plane wave for its proper functioning. The layout of the designed tag is depicted in Fig. 20. The substrate area measures 240 mm², with a length (L) of 16 mm and a width (W) of 15 mm.

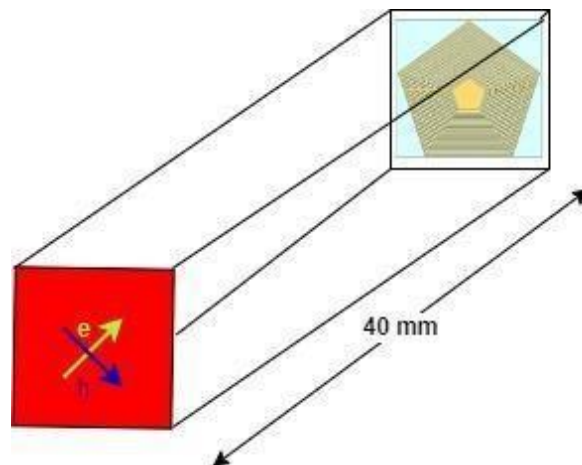


Fig. 3.2. Arrangement of tag in simulation setup

Throughout the design, a uniform width (d) of 0.2 mm is maintained for both the metallic portions and slots, ensuring ease of fabrication. The metallic portions C1 and C2, acting as dividers between the upper and lower halves of the tag, possess widths of 0.2 mm and 0.15 mm, respectively. The innermost pentagon's height is set at $H = 3.128$ mm. The data within

the tag is encoded using a slot resonator geometry, which comprises 29 slots of varying lengths. Each slot induces a dip or notch in the resonant frequency in the RCS plot, and these dips occur at distinct frequencies. Consequently, the presence of 29 dips allows the tag to represent 29 bits, thereby enabling it to label a total of 2^{29} (536,870,912) unique items.

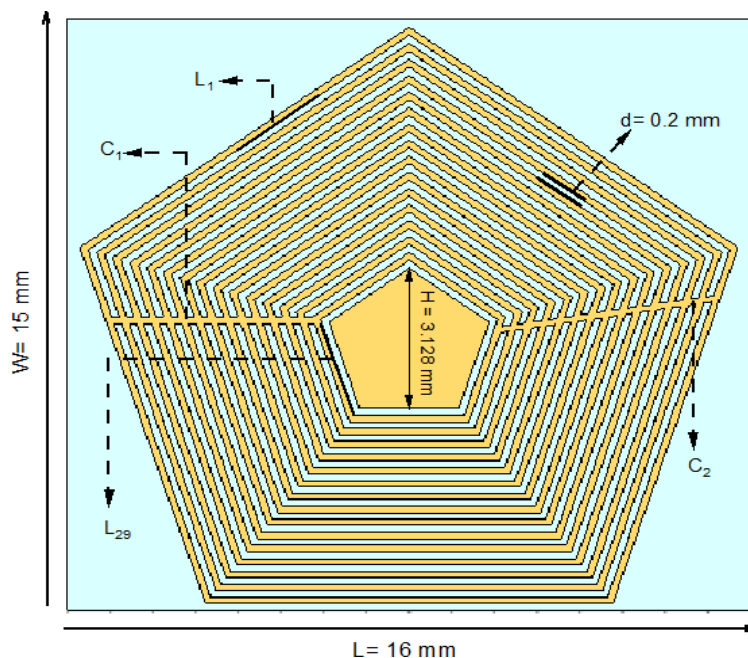


Fig. 3.3 Layout of the proposed tag

The slots from L_3 to L_{29} have been arranged in a pattern that ensures a minimum separation of $d = 0.2 \text{ mm}$ between each slot. This deliberate spacing helps to mitigate the mutual coupling effect that may occur among adjacent resonators. The specific measurements that define the tag's structure are provided in Table 1 for reference.

The slot-resonator configuration present on the tag's surface facilitates the backscattering process by ensuring that each resonant element is tuned to vibrate at a distinct frequency [35]. In this arrangement, every slot corresponds to a specific dip in the tag's frequency response, where each dip represents a single bit of information. The relationship between the resonant frequencies associated with a particular slot is expressed by equation (5):

$$f_r \approx \frac{c}{2L\sqrt{\epsilon_r}} \quad (5)$$

$$\text{where } \epsilon_{eff} = \frac{1 + \epsilon_r}{2}$$

Here, c represents the speed of light ($c = 3 \times 10^8$), L denotes the slot length, ϵ_{eff} stands for the

effective permittivity, and ϵ_r indicates the relative permittivity of the substrate. However, it's

important to note that this equation does not consider the impact of slot width and substrate thickness on the resonant frequency. The unit element design, as depicted in Fig. 23, serves as a foundation for constructing a multi-resonant data encoding structure.

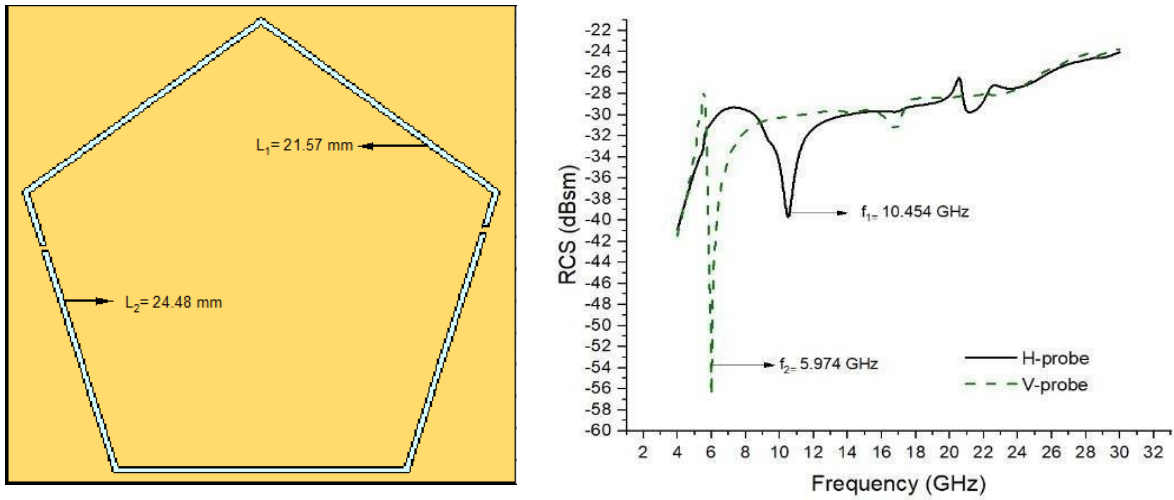


Fig. 3.4 (a) a single pentagon loop that has been diagonally cut to create two slots (b) the radar cross-section displaying frequencies associated with the lengths L_1 and L_2 .

Parameter	Length (mm)	Parameter	Length (mm)	Parameter	Length (mm)
$L1$	21.57	$L11$	15.73	$L21$	9.90
$L2$	24.48	$L12$	18.28	$L22$	12.11
$L3$	20.40	$L13$	14.55	$L23$	8.74
$L4$	23.24	$L14$	17.04	$L24$	10.87
$L5$	19.26	$L15$	13.42	$L25$	7.56
$L6$	22.03	$L16$	15.83	$L26$	9.62
$L7$	18.06	$L17$	12.24	$L27$	6.43
$L8$	20.76	$L18$	14.58	$L28$	8.41
$L9$	16.89	$L19$	11.07	$L29$	12.81
$L10$	19.52	$L20$	13.34		

Table 1. Dimensions of the slot resonator structure

3.2.1 Surface Current Distribution

There is another way to calculate the resonant frequency of a slot using its inductance and capacitance. When the reader emits an RF wave directed at the tag, an EM wave propagates within the structure. This, in turn, triggers a current distribution in the tag, leading to its excitation. The current distribution of the smallest slot has been simulated and visualized in Fig. 24. Additionally, Fig. 25 (a) offers a magnified view of the tag structure, highlighting the corresponding LC circuit of the slot.46+

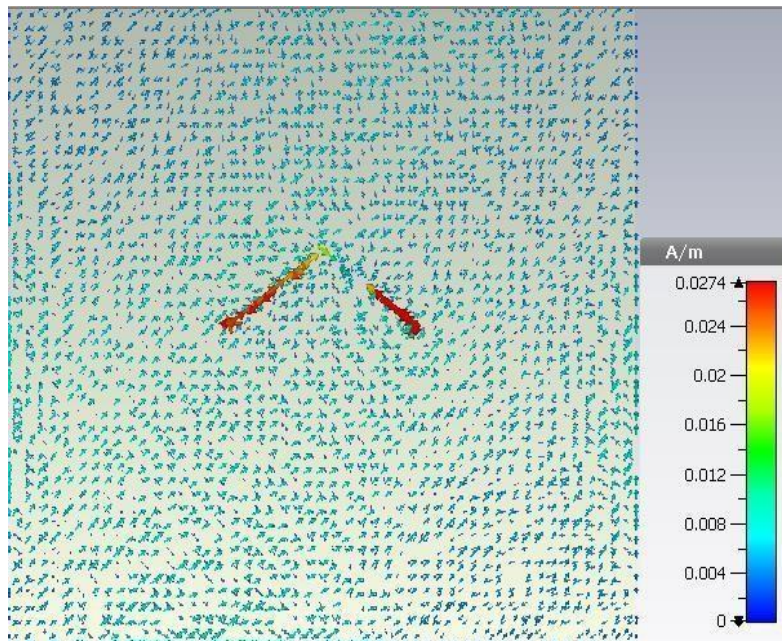


Fig. 3.5 Surface current distribution of the slot resonating at 28.87 GHz.

Upon plotting the series RLC circuit, it is observed that the capacitance increases while the inductance decreases. These changing values intersect at a particular frequency labeled as 'fr' in Fig. 25 (b). At this juncture, the inductance (X_L) and capacitance (X_C) achieve equilibrium ($X_L = X_C$), resulting in resonance at a specific frequency defined by equation (6).

$$fr = \frac{1}{2\pi\sqrt{LC}} \quad (6)$$

In this equation, 'fr' represents the resonant frequency, 'L' denotes the inductance, and 'C' signifies the capacitance of the circuit.

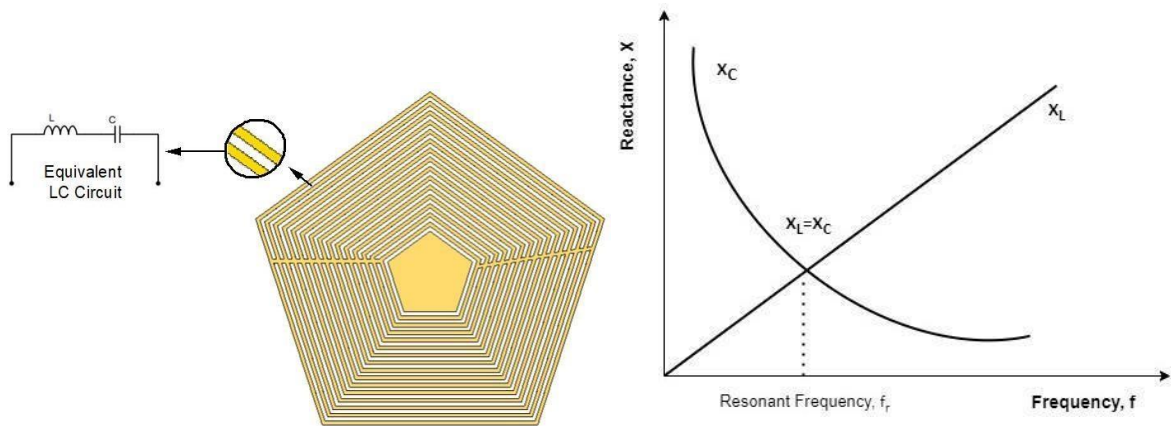


Fig. 3.6 (a) The equivalent series circuit of the shortest slot (b) Reactance vs. Frequency plot for the given equivalent circuit

3.3 Humidity Sensor

To introduce humidity sensing capabilities into the proposed tag, two options are considered: using Kapton[®]HN as the substrate or placing it over a specific slot in the tag structure. For this research, a thin film of Kapton[®]HN with a thickness of 0.1 mm is applied over the longest slot of the proposed tag, which resonates at 5.48 GHz, as shown in Fig. 26. The sensing bit is associated with the Most Significant Bit (MSB) of the tag, while the remaining 28 slots are dedicated to data encoding. The Kapton[®]HN film possesses the ability to absorb moisture from the surrounding atmosphere, leading to changes in its electrical properties. Consequently, these changes cause a shift in the overall frequency band of the tag. This alteration in frequency provides a means for detecting and quantifying humidity levels in the tag's environment [36,37].

By employing this innovative approach, the tag becomes more than just a data encoding mechanism; it transforms into a multifunctional sensor that can provide valuable insights into the humidity conditions of its surroundings. This integration of humidity sensing functionality within the tag extends its utility to applications in environmental monitoring, agriculture, and other fields where humidity plays a critical role.

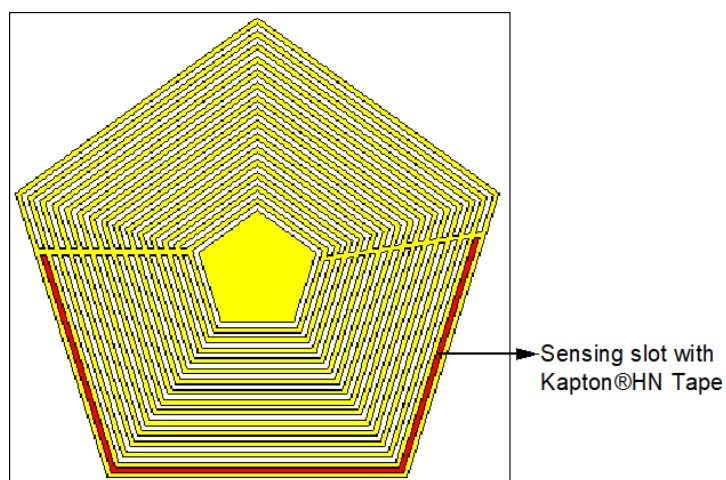


Fig. 3.7 Rogers RT/duroid® 5880 tag equipped with a Kapton®HN film, which is deposited over the longest slot.

Kapton®HN, a hygroscopic polymer, possesses a unique property of displaying a linear variation in its dielectric permittivity in response to changes in RH. The data sheet [38] reveals that the dissipation factor of Kapton®HN ranges from 0.0015 at 0% RH to 0.0035 at 100% RH. This characteristic behavior of Kapton®HN is represented by equation (7):

$$\epsilon_r = 3.05 + 0.008 \times \text{RH}\% \quad (7)$$

The chemical structure of Kapton®HN ($\text{C}_{12}\text{H}_{12}\text{N}_2\text{O}$) is depicted in Fig. 27. When Kapton®HN encounters water, a hydrolysis process occurs, wherein water molecules are absorbed into the free spaces within the polymer's structure. This phenomenon contributes to the change in the dielectric properties of Kapton®HN as a result of humidity absorption. The linear relationship between dielectric permittivity and relative humidity allows for a straightforward calibration of the tag's frequency response with respect to varying humidity levels. By monitoring the shift in resonant frequency due to changes in dielectric permittivity, the tag can accurately and quantitatively measure the surrounding humidity conditions.

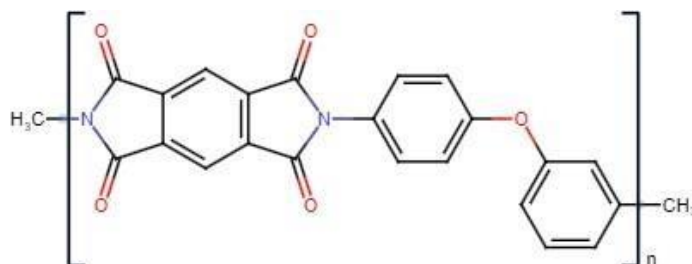


Fig. 3.8 Chemical structure of a Kapton®HN molecule

The variation in internal electric polarization occurs in Kapton[®]HN due to the breakdown of carbon-nitrogen bonds. When the polymer absorbs humidity, it experiences changes in permittivity, and this change is directly linked to the amount of water absorbed [39]. As a consequence of this alteration in permittivity, the electrical polarization within the material is modified, resulting in a shift in the resonant frequency of the tag.

The exceptional moisture-sensing capabilities of Kapton[®]HN polyamide make it highly suitable for deployment in various applications where moisture sensitivity is critical. Specifically, it proves to be an excellent choice for use in cold storages within the food industry, drug storage facilities, and other environments where maintaining optimal humidity levels is essential. In cold storages, the tag's ability to detect and respond to fluctuations in humidity levels ensures that food products remain properly preserved and safeguarded against spoilage. Likewise, in drug storage settings, where humidity control is vital for preserving the efficacy of medications, the Kapton[®]HN-deposited tag plays a crucial role in ensuring the quality and effectiveness of pharmaceutical products.

3.4 Temperature Sensor

The chipless design under consideration has been enhanced to include temperature sensing capabilities by introducing a temperature-sensitive material into a specific bit of the tag. This addition necessitated structural modifications within the tag architecture. To achieve temperature sensing functionality, the longest slot of the tag was modified to accommodate Stanyl[®]TE200F6 polyamide, a temperature-dependent polyamide, as illustrated in Fig. 28.

Stanyl[®] polyamide is renowned for its exceptional thermal expansion coefficient of (0.2 x 10⁻⁴ ppm/°C) [40], making it highly responsive to temperature changes. This unique property allows the tag to accurately detect and respond to variations in temperature levels. Moreover, Stanyl[®] polyamide exhibits remarkable resilience even in extreme temperatures and harsh environmental conditions. It can withstand high levels of stress and heavy loads without compromising its performance, rendering it highly reliable for temperature sensing applications.

By integrating Stanyl[®]TE200F6 polyamide into the tag's design, the chipless RFID tag transforms into a versatile sensor capable of accurately measuring temperature fluctuations. This newfound functionality opens up a multitude of applications in industries where

temperature monitoring is critical, such as automotive, aerospace, industrial processes, and other environments where precise temperature control is essential for optimal performance and safety.

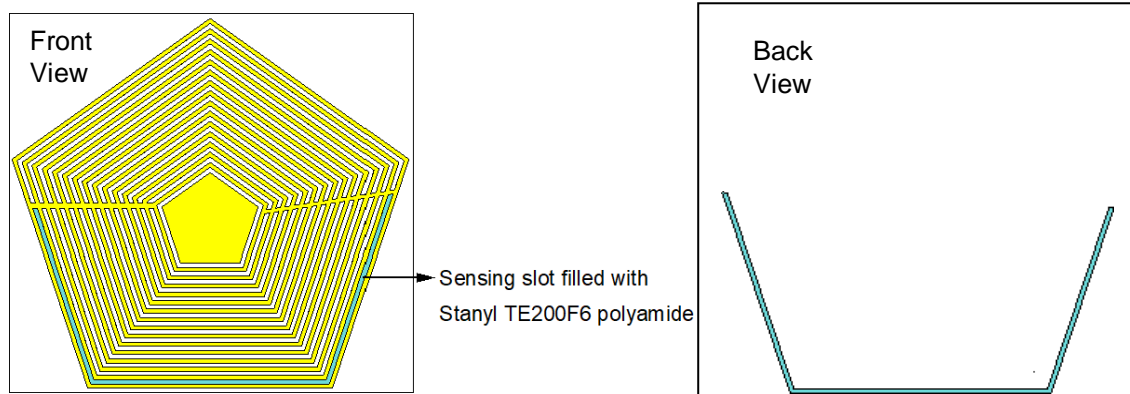


Fig. 3.9 Front and back view of the temperature sensing RFID tag

RESULTS AND DISCUSSIONS

4.1 Proposed Tag Analysis

The primary goal in developing the chipless RFID tag is to create a cost-effective and easily printable solution. To achieve this, the tag design mechanism has been carefully crafted to maintain simplicity and efficiency. Various substrates and conducting materials have been meticulously utilized in the design process to ensure the tag's practicality and affordability. The tag comprises a total of 29 bits, with fourteen bits observed through the upper slots, stimulated by horizontally polarized incident plane waves. In contrast, the remaining fifteen bits are observed through the lower slots, energized by vertically polarized RF waves. This dual-polarized configuration allows for efficient encoding and decoding of data, enabling the tag to represent a wide range of information in response to distinct frequencies within the specified range.

4.1.1 Tag-A

In the initial development, Tag-A was created using a flexible substrate known as Rogers RT/duroid®5880, incorporating copper resonators with a thickness of 0.35 mm. The substrate has a relative permittivity of 2.2, a thickness of 0.508 mm, and a low loss tangent of 0.0009. Fig. 29 illustrates the RCS response of the tag when an all-ones ID is applied. Each dip within the frequency range of 23.39 GHz correspondsto a '1' bit in the Tag ID. Notably, the MSB exhibits resonance at 5.48 GHz, while the LSB resonates at 28.87 GHz.

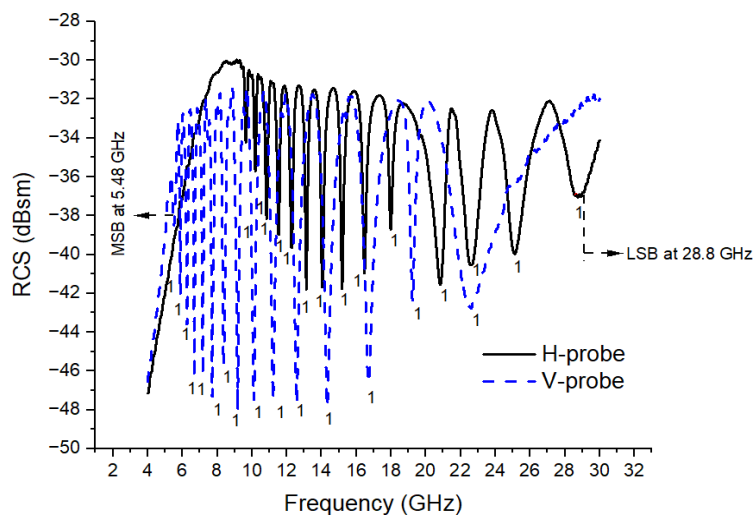


Fig. 4.1 RCS response of tag designed using Rogers RT/duroid® 5880 substrate.

4.1.2 Tag-B

The tag referred to as Tag- B is examined using a rigid laminate, specifically Rogers RT/duroid[®] 5870, with copper employed as the metallic radiator. Rigid tags are well-suited for various industrial applications, particularly in scenarios where items like boxes, containers, and similar objects require tagging. The substrate utilized for this rigid tag possesses a thickness of 0.78 mm, a dielectric constant of 2.2, and a loss tangent value of 0.0009. The electromagnetic response of the tag is depicted in Fig. 30, covering a bandwidth of 22.42 GHz with MSB resonating at 5.34 GHz and LSB at 27.76 GHz.

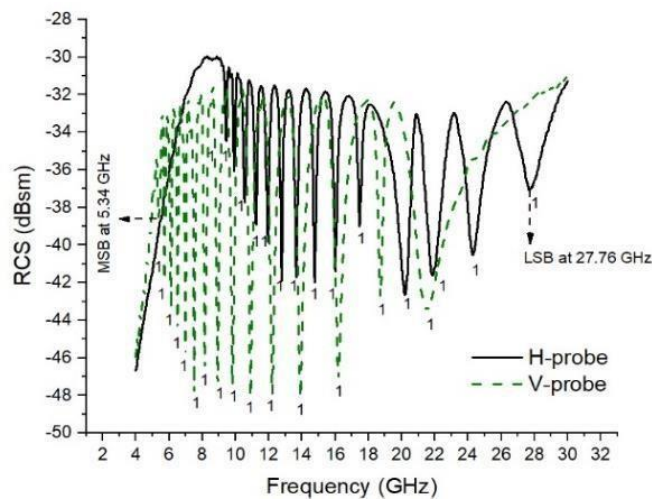


Fig. 4.2 RCS response of tag designed using Rogers RT/duroid[®] 5870 substrate.

4.1.3 Tag-C

An identical prototype has been implemented on a different rigid substrate called Taconic TLX-0. This substrate has specific properties, including a thickness of $h=0.635$ mm, a relative permittivity of $\epsilon_r=2.45$, and a loss tangent of $\tan \delta=0.0019$. Copper is utilized as the conductive material in this implementation. The simulated outcome of the tag can be observed in Fig. 31. This tag covers a bandwidth of 21.92 GHz, with MSB at 5.18 GHz and LSB (Least Significant Bit) at 21.1 GHz. With a thickness of $h=0.635$ mm, TLX-0 is a thin and lightweight substrate. This makes it suitable for applications where space and weight constraints are critical factors, such as in small RFID tags that need to be attached to various objects or products. Taconic TLX-0 is known for its stability and rigidity, which provides mechanical support and

protection for the delicate electronic components of the RFID tag. This ensures the tag's durability and robustness in different environmental conditions.

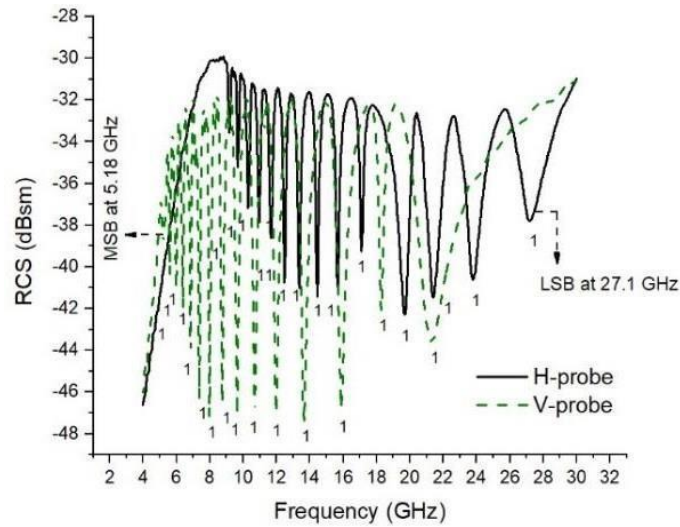


Fig. 4.3 RCS response of tag designed using Taconic TLX-0 substrate.

4.1.4 Tag-D

Tag-D is assessed using Kapton[®]HN as the substrate material, coupled with an Aluminum metal radiator with a thickness of 0.007 mm. The Kapton[®]HN substrate has a thickness of 0.125 mm, a relative permittivity value of 3.5, and a loss tangent of 0.0026. Fig. 32 showcases the RCS response of Tag-D, specifically for an all-ones ID combination. The operational frequency of this tag covers a range from 5.56 GHz to 28.75 GHz. Moreover, the MSB resonates at 5.56 GHz, while the LSB resonates at 28.75 GHz. The key electrical properties of Kapton[®]HN that are affected by humidity are its relative permittivity and loss tangent. Using Kapton[®]HN as a substrate for the development of chipless RFID tags turns the tag into a humidity sensor due to these properties of the Kapton material.

4.1.5 Tag-D'

The tag-D, designed using Kapton[®]HN as the substrate, incorporates conductive traces made from a silver nano-particle-based ink with a thickness of 0.015 mm. The RCS curve of this tag is displayed in Fig. 33. Within a bandwidth of 23.07 GHz, the tag achieves 29 bits of data encoding, with MSB resonating at 5.50 GHz and LSB resonating at 28.81 GHz. The ink's nanoscale particles allow for high-resolution printing of conductive traces, enabling the creation of intricate and precise tag

designs. This enhances the tag's readability. The ink-based fabrication process allows for scalable and reproducible production of chipless RFID tags.

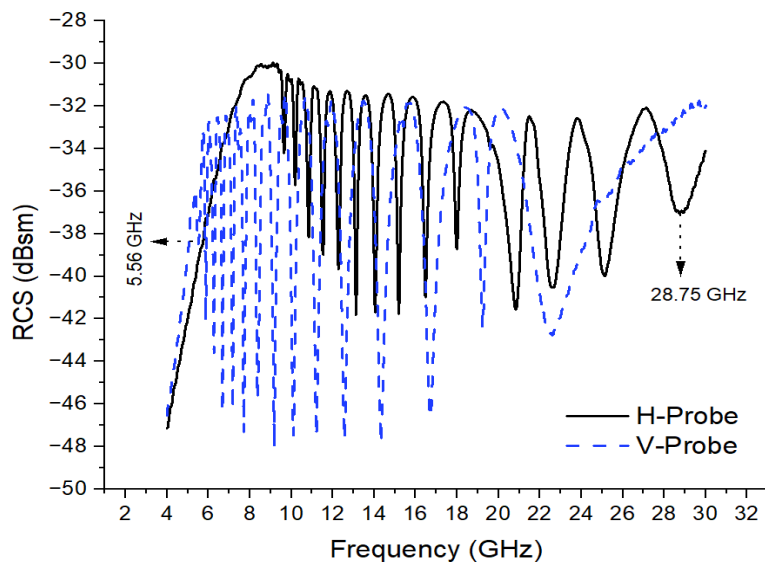


Fig. 4.4 RCS response of tag designed using Kapton[®]HN substrate with Aluminum resonators.

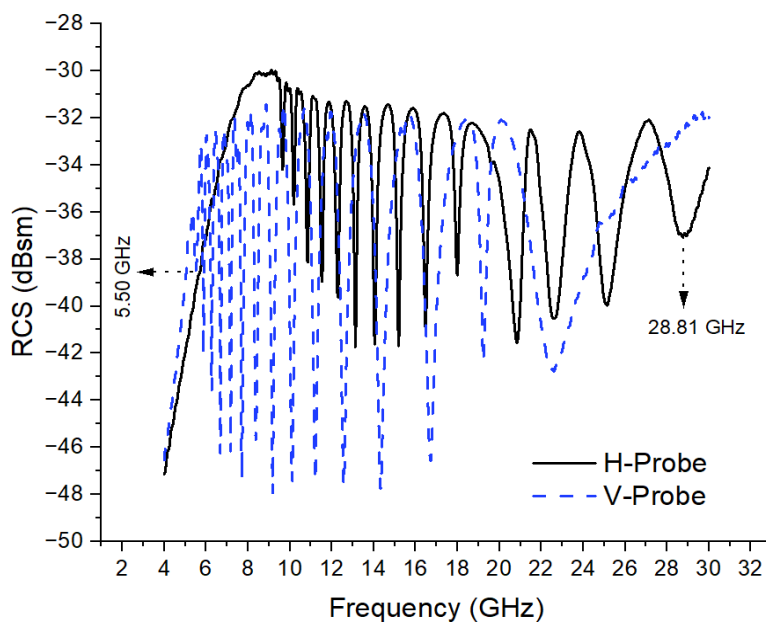


Fig. 4.5 RCS response of tag designed using Kapton[®]HN substrate with silver nanoparticle-based ink as radiator.

4.1.6 Tag-E

Tag-E is designed using a thin and flexible PET substrate. The PET substrate has a thickness of 0.1 mm and demonstrates specific electrical properties, including an

electric permittivity value of 3.3 and a loss tangent of 0.003. This tag uses Aluminum as the conducting material with a thickness of 0.007 mm. Fig. 34 provides a visual representation of the overall bandwidth achieved by Tag-E, which spans 23.32 GHz. The MSB resonates at 5.50 GHz, while the LSB resonates at 28.82 GHz.

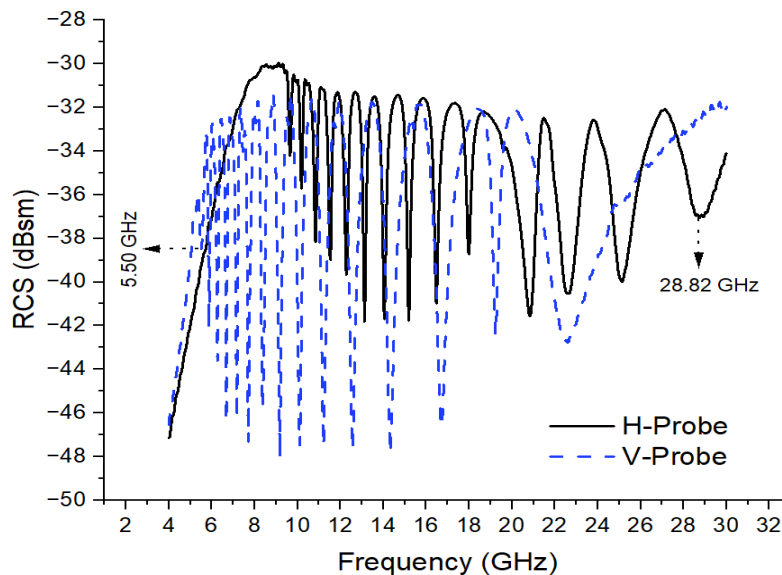


Fig. 4.6 RCS response of tag designed using PET substrate with Aluminum resonators.

4.1.7 Tag-E'

Fig. 35 depicts the frequency response of Tag-C', showing the RCS with respect to frequency. This RFID tag is manufactured using a PET substrate and incorporates silver nanoparticle-based ink as the radiating material. To simplify the fabrication process, the traditional Aluminum metal is replaced with a conductive ink, which has a thickness of 0.015 mm and exhibits excellent electrical conductivity, measuring 9×10^6 S/m. Tag-C' operates within a bandwidth ranging from 5.73 GHz to 29.73 GHz. A comprehensive comparison of the characteristics of the proposed tags is provided in Table 2.

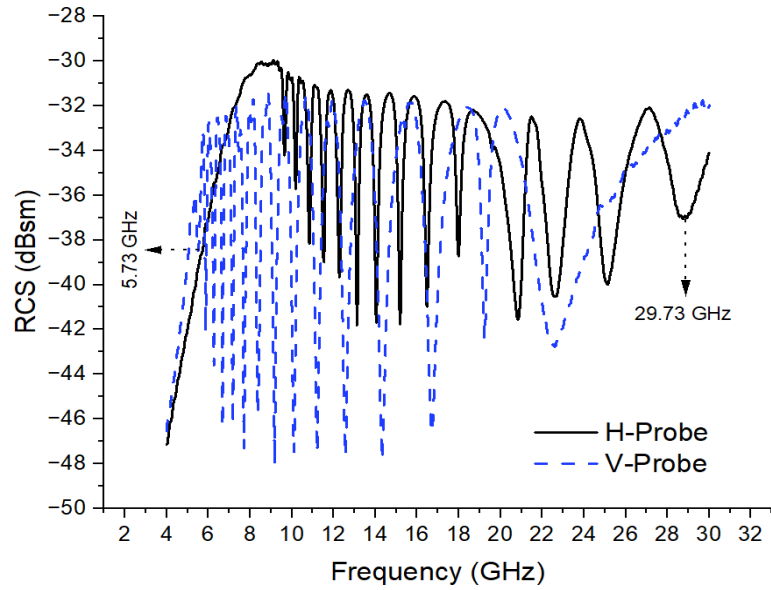


Fig. 4.7 RCS response of tag designed using PET substrate with silver nanoparticle-based ink as radiator.

4.1.8 Comparison of the Tags Designed

Table 2 provides a comprehensive comparison of the seven different tags that were designed during the research phase. These tags exhibit variations in their electrical properties and thickness, which directly impact their performance characteristics. Consequently, the bandwidth of each tag varies accordingly. The diversity in the tags' electrical properties and physical dimensions allows for a wide range of operational frequencies and data encoding capacities. Depending on the application requirements and specific frequency bands of interest, different tags can be selected.

Characteristics	Tag A	Tag B	Tag C	Tag D	Tag D'	Tag E	Tag E'
Laminate	RT/duroid5880	RT/duroid5870	Taconic TLX-0	Kapton®HN	Kapton®HN	PET	PET
Thickness (mm)	0.508	0.78	0.635	0.125	0.125	0.1	0.1
Permittivity	2.2	2.2	2.45	3.5	3.5	3.3	3.3
Loss tangent	0.0009	0.0009	0.0019	0.0026	0.0026	0.003	0.003
Radiator (µm)	Copper (35)	Copper (35)	Copper (35)	Al (7)	Silver (15)	Al (7)	Silver (15)
Bits	29	29	29	29	29	29	29 ^{jh}
Flexibility	✓	✗	✗	✓	✓	✓	✓
Spectral Band (GHz)	5.48 – 28.8	5.34 – 27.7	5.18 – 27.1	5.56 – 28.75	5.50 – 28.81	5.50 – 28.82	5.73 – 29.73

Table 2. Comparison table for the designed tags using different substrates.

4.2 Experimental Setup

The performance evaluation of the proposed RFID tag is carried out using an experimental setup similar to the one described in reference [41]. The setup includes a Vector Network Analyzer (VNA) equipped with two ports, with each port connected to a pair of identical horn antennas. One of the antennas functions as the transmitter, while the other serves as the receiver.

In this setup, the tag under test is affixed to a box and positioned in the far-field region relative to the horn antennas. The transmitter emits EM waves directed towards the tag. Upon interaction with the tag, it reflects a unique response onto the incident plane wave, which is then captured by the receiver. The backscattered encoded signal from the tag is fed back to the VNA for analysis of the transmitted and received response. The experimental setup illustrated in Fig. 36 demonstrates this procedure for testing and validating the performance of the proposed tag.

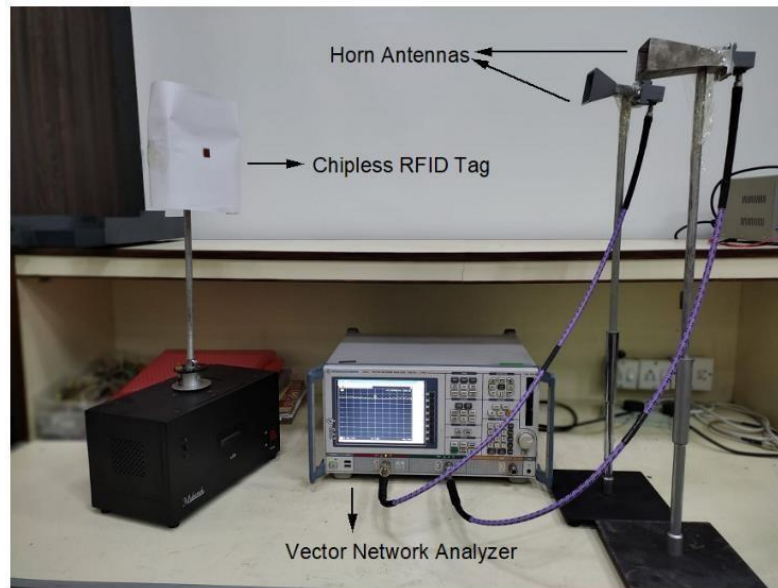


Fig. 4.8 The experimental setup for the proposed chipless RFID tag

When measuring the RCS response of the chipless RFID tag, two types of S_{11} parameters are obtained. The first parameter is $S_{11isolation}$, which is measured when the chipless tag is absent from the setup. The second parameter is S_{11ref} , which is measured with the chipless tag in place. To estimate the RCS value, equation (8) from reference [42] can be utilized:

$$\sigma_{tag} = \left[\frac{S_{11tag} - S_{11isolation}}{S_{11ref} - S_{11isolation}} \right]^2 \sigma_{ref} \quad (dBsm) \quad (8)$$

Here, σ^{tag} represents the RCS response of the chipless tag, while σ^{ref} denotes the RCS response of the proposed tag, as defined in equation (9):

$$\sigma^{\text{ref}} = \left[\frac{\text{Area of Plate}}{\lambda} \right]^2 4\pi \quad (9)$$

In Equation (9), λ represents the wavelength of the incident electromagnetic wave, and the "Area of Plate" is associated with the effective scattering area of the chipless tag.

The results obtained from both simulations and experimental measurements are presented in Fig. 37 and Fig. 38. It is noteworthy that the computed and measured results exhibit a considerable level of agreement, indicating the validity and accuracy of the proposed model in predicting the RCS response of the chipless RFID tag. The close correspondence between the simulated and measured data enhances confidence in the tag's performance.

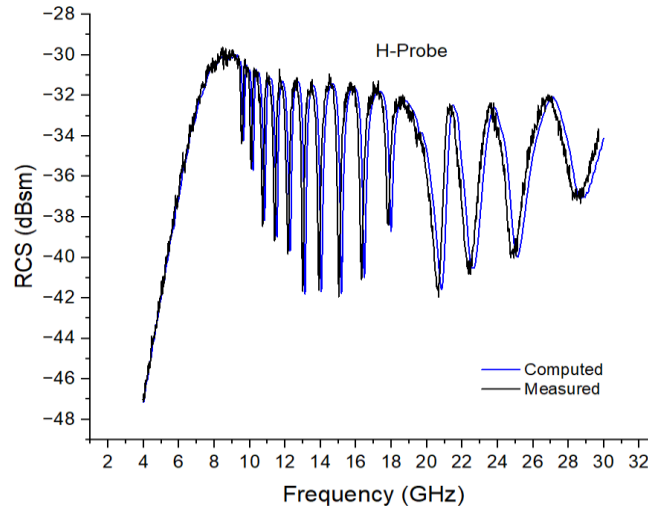


Fig. 4.9 Computed and measured results along H-probe

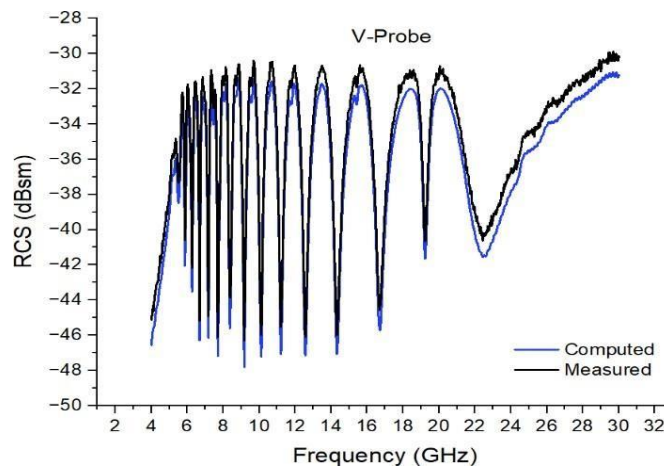


Fig. 4.10 Computed and measured results along V-probe

The results obtained from the measurements indicate that there is a slight deviation in the dips observed at certain resonant frequencies. This deviation can be attributed to a combination of environmental factors and minor design imperfections that may have occurred during the fabrication process. Environmental factors, such as variations in temperature, humidity, or electromagnetic interference in the testing environment, can influence the performance of the chipless RFID tag. These fluctuations may cause slight variations in the tag's electrical properties, leading to deviations in the resonant frequencies. Additionally, during the fabrication process, there might be subtle design disabilities or manufacturing imperfections that could impact the tag's performance. These imperfections could include variations in the thickness of the conducting material, alignment inaccuracies, or small defects in the substrate.

4.3 Multiple ID Combinations

The proposed prototype offers a high level of customization, enabling the encoding of distinct data words during the fabrication stage. Through the addition and removal of slots in the design, a remarkable variety of 2^{29} different tags can be generated, each possessing unique encoding capabilities. Fig. 39 showcases three examples of these unique tag variants. The first variant represents an all-ones combination, with a data word of 11111111111111111111111111111111. The second variant features an all-zero combination, with a data word of 00000000000000000000000000000000. Lastly, the third variant exhibits a random sequence with a data word of 10010010100110011000100010101. Each of these variants is depicted along with their physically altered structures, demonstrating how the addition or removal of slots results in specific encoding patterns. These alterations in the tag's physical structure correspond directly to the data word it represents. In Fig. 39 (a), no slot has been shorted. In Fig. 39 (b), all slots of the tag are shorted by filling the substrate material within the slots. In Fig. 39 (c), the slot numbers 2,4,6,7,8, 11, 12, 15, 16, 19, 20, 22, 24, 25, 27 and 28 are shorted. For the shorted slots, there are flat dips in the corresponding RCS response at those frequencies. The flexibility to create such a diverse range of tags provides valuable opportunities for tailoring RFID solutions to specific applications.

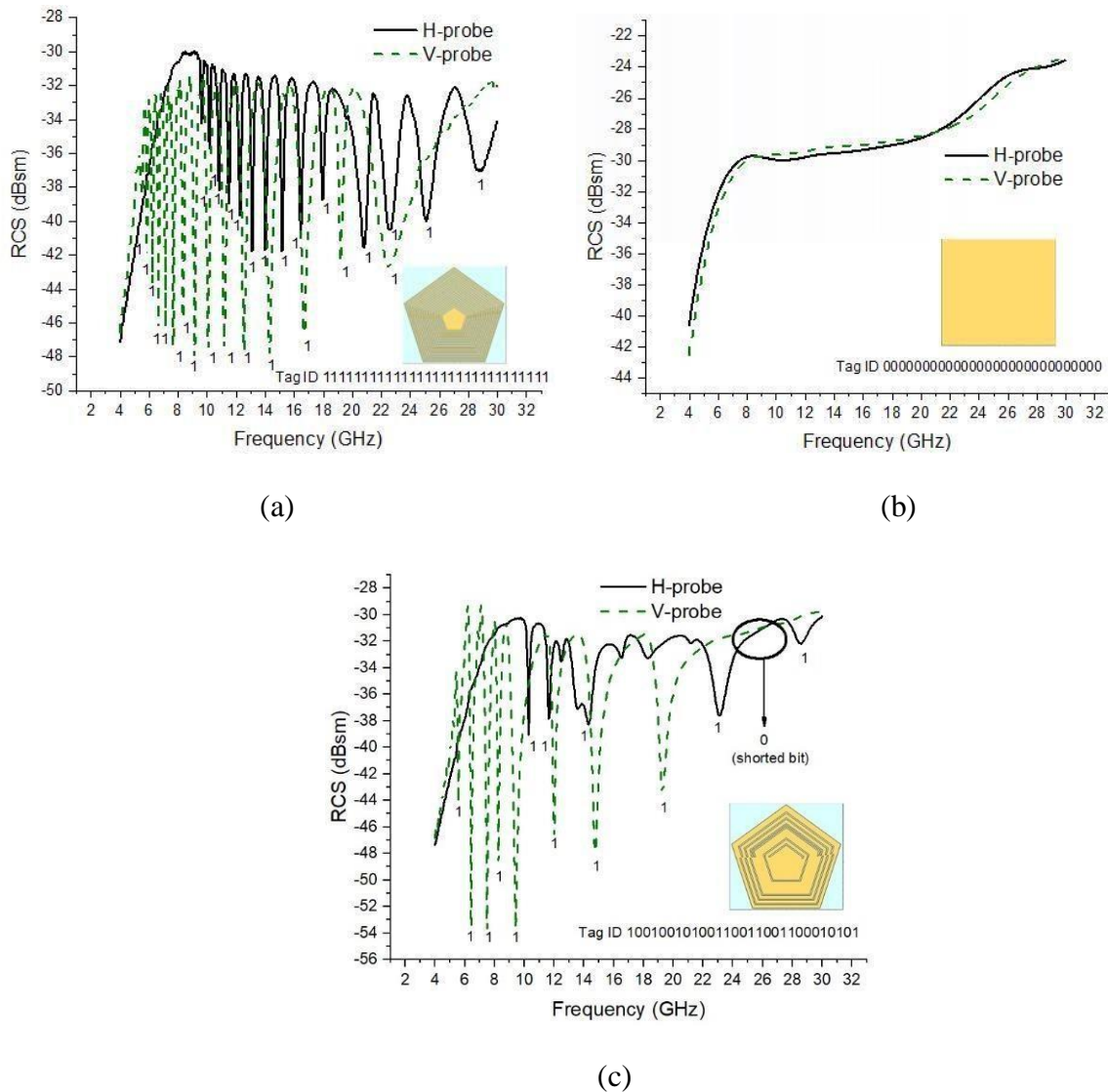


Fig. 4.11 RCS and tag design for data word 11111111111111111111111111111111 (b) RCS and tag structure for data word 00000000000000000000000000000000 (c) RCS and tag design for data word 10010010100110011000100010101

4.4 Humidity Sensing Behavior of the Tag

The quantification of the resonance shift of the tag's sensing slot in the presence of moisture is referred to as humidity sensing. Fig. 40 illustrates the humidity sensing characteristics of the tag on the H-probe under different humidity levels (30%, 50%, and 80%) for the tag presented in Fig. 26. The results demonstrate that as the RH increases, the permittivity of Kapton®HN changes from 3.3 to 3.7. This variation in permittivity leads to a corresponding shift in the resonant frequency of the sensing slot. Specifically, the resonant frequency moves towards lower frequencies as the humidity level rises. In essence, the tag's ability to detect and respond to changes in humidity levels is attributed to the interaction between the

moisture in the environment and the electrical properties of the Kapton[®]HN substrate. This phenomenon offers a valuable humidity sensing capability, making the tag a versatile and adaptable solution for applications where humidity monitoring is crucial.

A 20% increase in RH from 30% to 50% results in a frequency shift of 77.2 MHz in the RCS curve, while a further 20% rise from 50% to 80% leads to a frequency shift of 51.5 MHz towards the left side. It is essential to emphasize that these shifts in the resonating frequency of the sensing slot do not affect the number of bits generated by the tag.

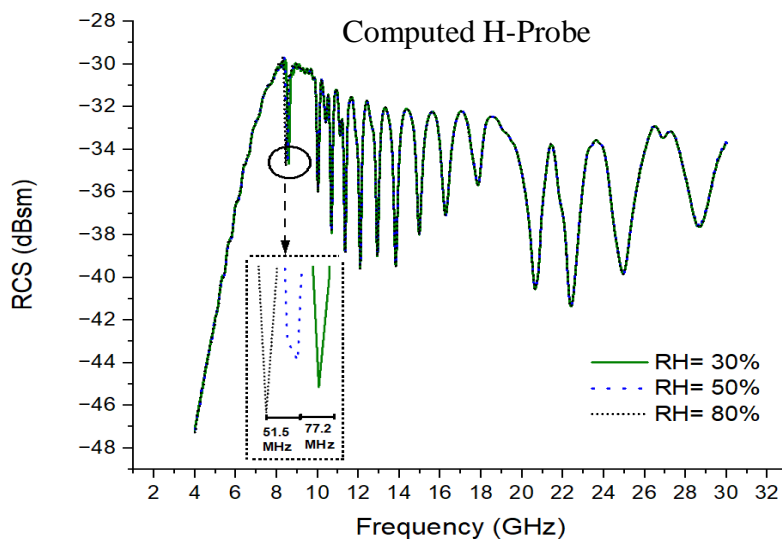


Fig. 4.12 Computed humidity sensing behavior of the proposed tag

To measure the response of the proposed humidity RFID sensor tag, a well-defined setup as outlined in [20] is utilized. The setup includes an environmental chamber with dimensions of 50 x 34 x 36 cm³, two horn antennas, a water spray bottle, a commercial sensor, and the proposed humidity sensor. The measurement process is conducted at room temperature, with a VNA positioned near the environmental chamber. Within the chamber, the horn antennas and sensor are positioned 20 cm above the bottom of the box, while the proposed humidity sensor tag is placed at a far-field distance of 40 mm from the horn antennas. The RCS is determined using equation (8). To simulate different humidity levels, the measurement process involves spraying water inside the airtight chamber and subsequently closing the lid for a duration of 10 minutes.

Fig. 41 presents the humidity response of the proposed sensor, showcasing measurements taken along horizontal probes. To acquire the measured results at different relative humidity (RH) levels of 30%, 50%, and 80%, water is periodically sprayed inside the chamber,

inducing variations in the moisture levels. Consequently, the thin Kapton[®]HN tape deposited on the longest slot of the tag undergoes changes in its electrical properties, leading to a drift of the MSB towards lower frequencies in the RCS response. These variations in the environmental moisture level are depicted as ripples in the measured response.

The observed shift in the MSB resonant frequency in the RCS response is significant, with a total shift of 128.7 MHz from 8.57 – 8.44 GHz when the relative humidity increases up to 80%. This shift can be attributed to the alterations in the permittivity of the Kapton[®]HN substrate, caused by the fluctuating moisture levels within the chamber.

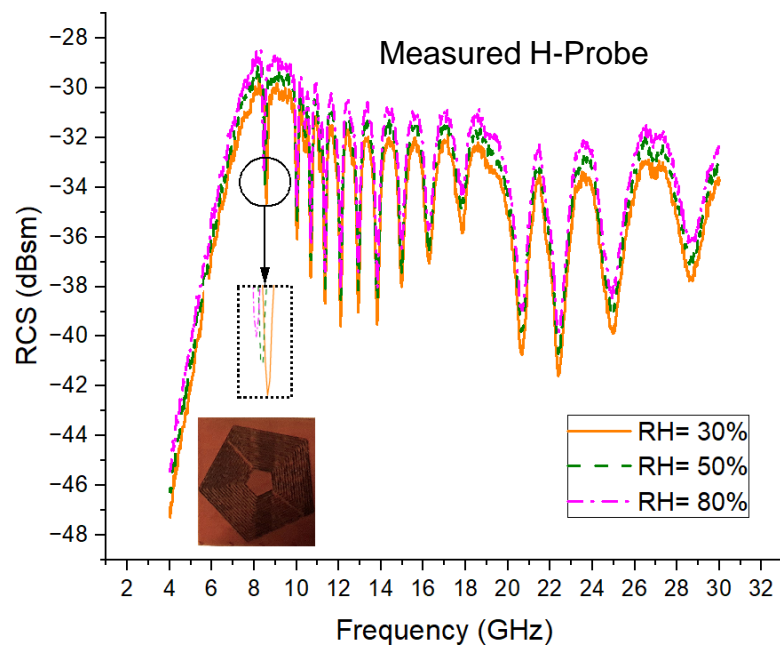


Fig. 4.13 Measured results of the humidity sensor.

These findings demonstrate the sensitivity of the proposed humidity sensor tag to changes in the surrounding humidity, making it a promising and reliable solution for humidity monitoring applications. The ability to detect and respond to environmental factors further enhances the tag's suitability for diverse practical scenarios where accurate humidity measurements are crucial.

4.5 Temperature Sensing Behavior of the Tag

Consider Fig. 28, a section with the same length as the longest slot is removed from the Rogers RT/duroid[®] 5880 substrate and replaced with Stanyl[®] polyamide. This alteration primarily affects the lowest resonant frequency within the tag's frequency signature, while the

neighboring resonant frequencies remain unaffected, preserving their role in data encoding. In Fig. 42, it is evident that as the relative permittivity (ϵ_r) increases from 3.5 to 3.8 due to a rise in temperature, there is a slight drift of 79.8 MHz towards lower frequencies in the resonant frequency of the sensing slot. This change in the resonant frequency provides valuable sensing information, which can be correlated with temperature variations.

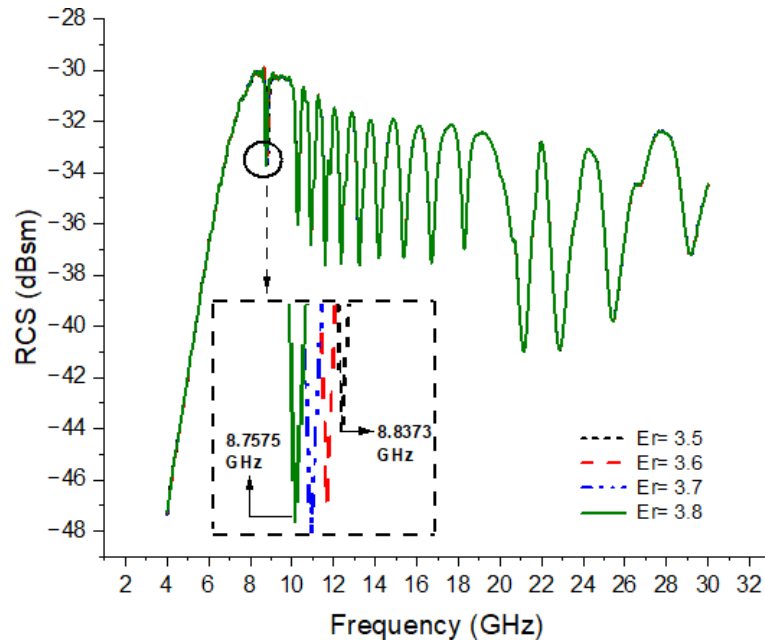


Fig. 4.14 Temperature sensing behavior of the proposed sensor tag

The obtained results highlight an inverse correlation between the resonant frequency and temperature. As the temperature increases, the resonant frequency of the sensing slot shifts towards lower frequencies. This behavior enables the proposed tag to act as a temperature sensor, where the shifting resonant frequency serves as an indicator of changes in the surrounding temperature. This temperature-sensing capability adds versatility to the tag's functionalities, making it suitable for a wide range of applications that require temperature monitoring and control. The tag's ability to respond to temperature variations enhances its utility accurately and reliably in various practical scenarios.

The experimental setup for testing the temperature sensing tag is the one used by N. Javed et al. in [20]. This setup includes an environmental chamber which comprises two horn antennas, an electronic commercial sensor, and the proposed sensor-embedded chipless RFID tag. This assembly is connected to a VNA. The chamber is injected with 20,000 ppm CO₂ concentration which raises the temperature inside the chamber. As the temperature increases, the dielectric constant of the substrate also varies. It is a good practice to place the sensor tag

to be tested over some surface like a wooden plank or cardboard to minimize the effect of ground reflections. Fig. 43 shows the measured results of the Stanyl® Polyamide filled chipless RFID sensor tag.

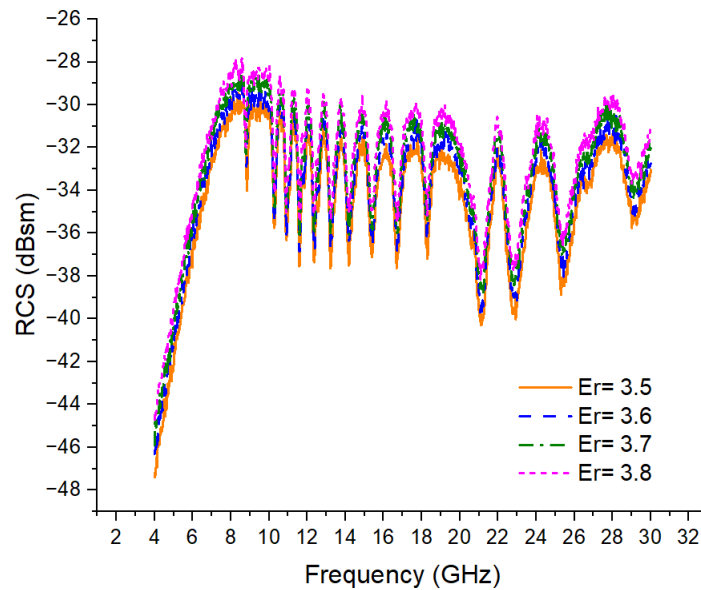


Fig. 4.15 Measured results of the temperature sensor on H-probe

In Fig. 44, an analysis is depicted, illustrating the connection between the dielectric constant and temperature. The results reveal a linear relationship, indicating that the Stanyl® polyamide material experiences predictable changes in its dielectric constant as the temperature varies [57]. As a consequence, the effective relative permittivity of the tag is influenced, causing a shift in its frequency response.

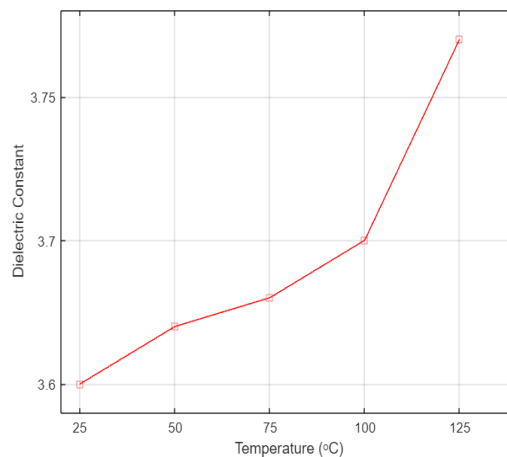


Fig. 4.16 Relationship between dielectric constant of Stanyl®TE200F6 and temperature.

4.6 Comparison with Previously Published RFID Tags

Table 3 provides a comparative analysis between the proposed chipless RFID tag and previously reported state-of-the-art tags. The table presents a comparison of various key parameters, highlighting the novelty of our work in relation to existing research. The proposed tag boasts several characteristic parameters that set it apart: high data density, flexibility, printability, high spectral capacity, and sensing capabilities. These attributes constitute the main strengths of our proposed tag, making it stand out in the field of chipless RFID technology. The realized sensor tag is based on stable and reliable materials, rendering it suitable for deployment in challenging and harsh environmental conditions. This robustness ensures the tag's performance remains consistent and dependable even in adverse settings. All these factors render the proposed tag a promising advancement in chipless RFID technology, addressing the limitations of previous designs and offering a more efficient and capable solution for diverse applications.

Ref.	Dimension (cm ²)	Bit Capacity (Bits)	Bit Density (Bits/cm ²)	Flexibility	Sensing	Frequency Band (GHz)
[43]	30.25	8	3.90	✓	☐	5 – 13
[44]	1.41	20	15.15	✓	☐	3 – 8
[45]	3.65	10	2.74	✓	☐	3.6 – 15.6
[46]	3.03	3	0.99	☐	✓	3.86 – 5.75
[47]	1.83	10	5.44	✓	☐	5.5 – 10.4
[48]	2.25	5	2.22	☐	☐	5.5 – 9.5
[49]	24.75	6	0.24	✓	✓	5.3 – 11
[50]	4.25	20	4.70	✓	✓	4.1 – 16
[51]	25	21	0.84	☐	☐	3 – 10
[52]	16.66	8	0.48	☐	☐	3 – 6
Proposed Work	2.40	29	12.08	✓	✓	5.48 – 28.87

Table 3. Comparison of the reported tag with previously reported tags

CONCLUSION AND FUTURE WORKS

5.1 Conclusion

This research presents a novel chipless RFID sensor tag that incorporates frequency domain-based encoding, enabling the tagging of an impressive 536,870,912 items. The tag's design has been meticulously engineered to achieve a compact size, measuring just 15 x 16 mm². A comprehensive analysis of the tag has been undertaken, considering its performance on five distinct substrates: Rogers RT/duroid/5880, Rogers RT/duroid/5870, Taconic TLX-0, Kapton[®] HN, and PET. These substrate variations offer valuable insights into the tag's behavior and suitability across diverse operating conditions.

Beyond its fundamental data storage capabilities, this tag incorporates advanced features for humidity and temperature sensing. To achieve humidity sensing, moisture-sensitive tape is thoughtfully integrated, allowing the tag to accurately monitor humidity levels in its surroundings. This feature is particularly advantageous in applications where maintaining optimal humidity conditions is critical, such as the storage of sensitive electronic components or perishable goods.

Temperature sensing, on the other hand, is enabled by integrating heat-sensitive Stanyl[®] polyamide within the longest slot of the tag. This material, known for its excellent thermal conductivity properties, empowers the tag to effectively sense temperature fluctuations. This aspect makes the tag highly suitable for applications where precise temperature control is essential, such as in cold chain logistics or temperature-sensitive manufacturing processes.

By incorporating both humidity and temperature sensing capabilities, the tag transforms into a versatile and comprehensive monitoring solution. Thus, it not only stores essential data but also provides valuable insights into the environmental conditions it operates within, ensuring optimal conditions and enhancing overall operational efficiency.

The tag's sensing behavior is observed in the MSB of the RCS response. To verify its performance, a meticulous comparison of computed and measured results is conducted, demonstrating excellent agreement between the two. These experimental results further affirm the efficacy of the proposed tag, showcasing its remarkable capabilities in unique identification and sensing performance.

In conclusion, this novel chipless RFID sensor tag offers unparalleled data storage capacity and advanced sensing functionalities. Its compact design, versatility, and reliable performance make it an invaluable asset in a wide range of applications, enabling efficient and accurate monitoring in various environmental conditions.

5.2 Trends in the RFID Market for 2023 and Beyond: A Five-Year Outlook

The RFID industry is experiencing ongoing expansion, and it is expected that the global RFID market will maintain its growth trajectory in 2023. According to IDTechEx's forecast, the market is poised to reach a value of US\$14 billion in 2023, marking an increase from the US\$12.8 billion recorded in 2022. This market valuation encompasses various RFID components such as labels, cards, fobs, and other physical formats, alongside tags, scanners, and software/services designed for both active and passive RFID technologies.

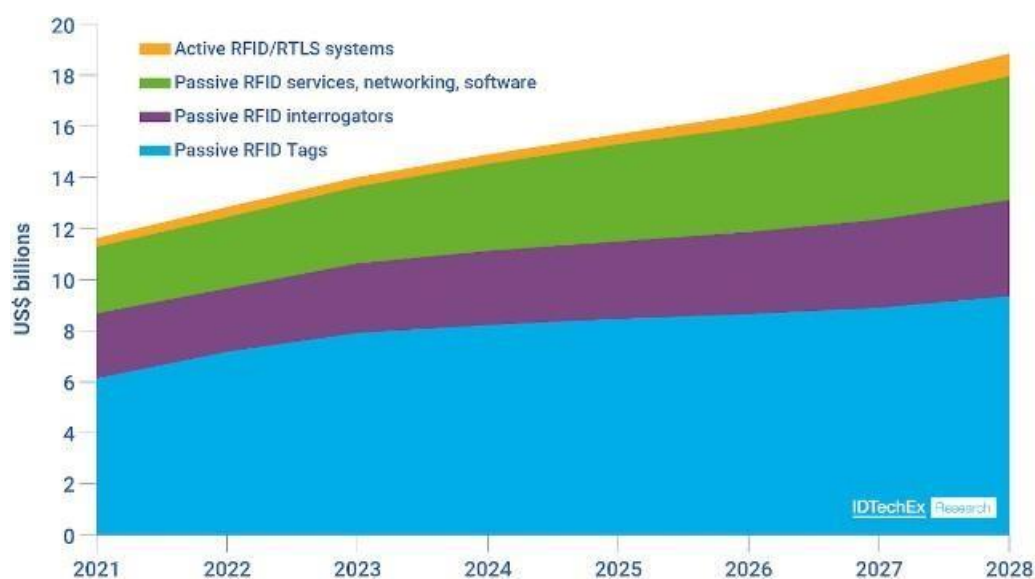


Fig. 5.1 Total RFID market size 2021-2028. Source: IDTechEx - "RFID Forecasts, Players and Opportunities 2023-2033"

It is noteworthy that the "Passive RFID Tags" segment commands a substantial share, constituting more than half of the total RFID market. According to the analysis presented in "RFID Forecasts, Players and Opportunities 2023-2033" by IDTechEx, there is a notable growth trend with 39.3 billion passive RFID tags projected to be sold in 2023, an increase from 33 billion in 2022, indicating robust double-digit growth primarily driven by passive UHF RFID tags.



Fig 5.2. Passive RFID tag market value by type in 2023 and passive RFID tag volume by type in 2023. Source: IDTechEx - "RFID Forecasts, Players and Opportunities 2023-2033"

Retail apparel continues to maintain its dominant position within the UHF RFID sector, both in terms of the sheer quantity of tags deployed and its overall market size. As per IDTechEx's projections, the usage of RFID labels in retail apparel tagging is expected to reach nearly 24 billion by 2023. However, it's important to note that this substantial number, impressive as it may seem, accounts for only 30% of the total potential market for RFID tagging in the retail apparel sector alone.

While the retail apparel industry has undeniably achieved notable success, IDTechEx foresees robust growth potential in another arena—namely, the tagging of various other retail products such as electronics, soft furnishings, home appliances, and more. Valuable insights gathered through interviews conducted by IDTechEx reveal that Walmart's directive plays a pivotal role in driving this expansion. In addition to the retail sector, the supply chain and logistics industry is also experiencing significant interest and investment, demonstrating steady growth in response to market demand.

While the RFID market maintains its upward trajectory, it grapples with persistent challenges. The global supply chain disruption that began in 2021 lingers, albeit with less severe repercussions than before. Due to the global economic deceleration, certain sectors have curtailed their RFID tag purchases, potentially dampening the pace of growth. Another enduring concern is the fragmented nature of the RFID ecosystem across numerous sectors, a matter that necessitates attention for widespread RFID adoption to occur.

In contrast, the success of retail apparel tagging can be attributed to its well-established and stable solution ecosystem. Moreover, addressing issues related to education, regulation, and cost reduction remains imperative for RFID stakeholders as they navigate the evolving landscape.

5.3 Future Works

Several potential future works and developments can be explored for the proposed chipless RFID sensor tag to enhance its capabilities and applicability. Some possible avenues for future research include:

- **Multi-Sensor Integration:** Explore the integration of additional sensors into the tag to enable multi-parameter sensing. This could involve incorporating sensors for pressure, light, gas, or other environmental parameters, providing a comprehensive and versatile monitoring solution for various applications.
- **Energy Harvesting:** Investigate the possibility of integrating energy harvesting mechanisms within the tag to enable self-powering capabilities. By harnessing ambient energy sources, such as solar, mechanical, or RF energy, the tag can become self-sustaining and prolong its operational lifespan.
- **Wireless Communication:** Explore the incorporation of wireless communication capabilities in the tag. This could enable real-time data transmission to centralized monitoring systems, enhancing remote monitoring and control capabilities in IoT and smart applications.
- **Enhanced Data Encryption:** Implement advanced data encryption techniques to ensure the security and privacy of sensitive information stored within the tag. This would be particularly relevant for applications where data security is of utmost importance.
- **Long-Range Sensing:** Investigate techniques to extend the sensing range of the tag. By increasing the tag's read range, it can be employed in scenarios requiring long-range monitoring, such as environmental monitoring or asset tracking.
- **Material Selection:** Explore alternative materials for the tag's construction to optimize its performance in specific environments or under extreme conditions.

Materials with superior durability, resistance to environmental factors, or unique sensing properties could be considered.

- **Energy-Efficient Sensing:** Research methods to optimize the tag's power consumption during sensing operations. Energy-efficient sensing techniques would ensure extended battery life or better energy harvesting performance.
- **Standardization and Interoperability:** Work towards standardizing the chipless RFID sensor tag to ensure compatibility with various systems and technologies. Standardization would foster wider adoption and seamless integration into existing infrastructures.
- **Field Trials and Validation:** Conduct field trials and validation studies in real-world environments to assess the tag's performance and reliability under practical conditions. Field tests would provide valuable insights for further optimization and refinement.

BIBLIOGRAPHY

- [1] Crepaldi, Paulo & Pimenta, Tales. (2017). Introductory Chapter: RFID: A Successful History. 10.5772/intechopen.69602.
- [2] It's Shocking How Well This RFID Pioneer Predicted the Future: <https://www.zebra.com/us/en/blog/posts/2023/it-is-shocking-how-well-rfid-pioneer-mario-cardullo-predicted-the-future.html>
- [3] Eleonora Bottani, Antonio Rizzi, (2008) "Economical assessment of the impact of RFID technology and EPC system on the fast-moving consumer goods supply chain", Journal of Production Economics, Volume 112, Issue 2, Pages 548-569.
- [4] Kim and H. Li, (2011). 'Fabrication and Applications of Carbon Nanotube-Based Hybrid Nanomaterials by Means of Non-Covalently Functionalized Carbon Nanotubes', Carbon Nanotubes - From Research to Applications. InTech. (doi: 10.5772/18002.
- [5] Eteng, Akaa & Abdul Rahim, Sharul & Leow, Chee Yen. (2018). RFID in the Internet of Things: Technologies and Applications. 10.1002/9781119456735.ch5.
- [6] Gouse Baig Mohammad, Shitharth Shitharth, Salman Ali Syed, Raman Dugyala, K.Sreenivasa Rao, Fayadh Alenezi, Sara A Alhubiti, Kemal Polat, (2022). "Mechanism of Internet of Things (IoT) Integrated with Radio Frequency Identification (RFID) Technology for Healthcare System", Mathematical Problems in Engineering, vol. 2022, Article ID 4167700, 8 pages. <https://doi.org/10.1155/2022/4167700>
- [7] Technology status and application development: ESSCIRC 2008-34th European Solid-State Circuits Conference. IEEE, 2008.

- [8] Khan, Yasser & Thielens, Arno & Muin, Sifat & Ting, Jonathan & Baumbauer, Carol & Arias, Ana. (2020). A New Frontier of Printed Electronics: Flexible Hybrid Electronics. *Advanced Materials*. 32. 10.1002/adma.201905279.
- [9] E. Welbourne, L. Battle, G. Cole, K. Gould, K. Rector, S. Raymer, M. Balazinska, and G. Borriello, (2009). "Building the internet of things using RFID: the RFID ecosystem experience," *Internet Computing*, IEEE, vol. 13, no. 3, pp. 48-55.
- [10] L. Yan, Y. Zhang, and L. T. Yang, (2008). "The Internet of things: from RFID to the next-generation pervasive networked systems", Auerbach Pub.
- [11] Daniel M. Dobkin. (2007). *The RF in RFID: Passive UHF RFID in Practice*. Newnes, USA.
- [12] Yoon, W.-J., Chung, S.-H., Lee, S.-J., & Moon, Y.-S. (2007). Design and Implementation of an Active RFID System for Fast Tag Collection. 7th IEEE International Conference on Computer and Information Technology (CIT 2007). doi:10.1109/cit.2007.31
- [13] Tanim, M M Zaman. (2016). How does passive RFID works, briefly explained.10.13140/RG.2.2.12361.34402.
- [14] Aigner, M.J., Plos, T., Coluccini, S., & Ruhanen, A. (2008). D4.2.2 Secure Semi-Passive RFID Tags – Prototype and Analysis.
- [15] Sabri Serkan Basat, (2006). "Design and characterization of rfid modules in multilayer configurations", Georgia Institute of Technology.
- [16] Botao Shao, (2014). "Fully printed chipless RFID tags towards item-level tracking applications", Stockholm, Sweden.
- [17] C. A. Valhouli, (2010). "The Internet of things: Networked objects and smart devices," The Hammersmith Group research report, pp. 1-7.

- [18] Khan, Ameer & Abdullah, Yassin & Farhat, Sidra & Nawaz, Wasim & Rouf, Usman. (2020). Design and analysis of truncated elliptical shaped chipless RFID tag. *Turkish Journal of Electrical Engineering and Computer Sciences*.
- [19] Aslam, Bilal & Azam, Muhammad Awais & Amin, Y. & Loo, Jonathan & Tenhunen, Hannu. (2019). A high-capacity tunable retransmission type frequency coded chipless radio frequency identification system. *International Journal of RF and Microwave Computer-Aided Engineering*. 29. e21855. 10.1002/mmce.21855.
- [20] N. Javed, M. A. Azam, I. Qazi, Y. Amin and H. Tenhunen, (2020). "Data-Dense Chipless RFID Multisensor for Aviculture Industry," in *IEEE Microwave and Wireless Components Letters*, vol. 30, no. 12, pp. 1193-1196. doi: 10.1109/LMWC.2020.3032027.
- [21] Jabeen, Iqra & Ejaz, Asma & Akram, Adeel & Amin, Y. & Loo, Jonathan & Tenhunen, Hannu & Amin, Y.. (2019). Elliptical slot based polarization insensitive compact and flexible chipless RFID tag. *International Journal of RF and Microwave Computer-Aided Engineering*. 10.1002/mmce.21734.
- [22] G. Khadka, M. A. Bibile, L. M. Arjomandi, et.al, (2019). "Analysis of Artifacts on Chipless RFID Backscatter Tag Signals for Real World Implementation", *IEEE Access*, vol. 7, pp. 66821-66831.
- [23] Tehmina & Khan, Ameer & Amin, Y. & Ahmad, Shakeel. (2021). RFID in IoT, Miniaturized Pentagonal Slot-based Data Dense Chipless RFID Tag for IoT Applications. *ARABIAN JOURNAL FOR SCIENCE AND ENGINEERING*. 47. 10.1007/s13369-021-06228-9.
- [24] Khan, Ameer & Riaz, Muhammad & Shahid, Humayun & Amin, Y. & Tenhunen, Hannu & Loo, Jonathan. (2021). "Design of a Cobweb Shape Chipless RFID Tag". *Microwave Journal*. 64. 90.

- [25] Javed, Nimra & Azam, Muhammad Awais & Amin, Y. (2021). Chipless RFID Multi-sensor for Temperature Sensing and Crack Monitoring in an IoT Environment. *IEEE Sensors Letters*. PP. 1-1. 10.1109/LSENS.2021.308321
- [26] Habib S, Ali A, Kiani GI, Ayub W, Abbas SM, Butt MFU (2021). A low-profile FSS-based high capacity chipless RFID tag for sensing and encoding applications. *International Journal of Microwave and Wireless Technologies* 1–9. <https://doi.org/10.1017/S1759078721000362>
- [27] A. Habib, et al. (2022). "Data dense chipless RFID tag with efficient band utilization." *AEU-International Journal of Electronics and Communications*, p.154220.
- [28] Ali, Amjad & Williams, Orla & Lester, Ed & Greedy, Steve. (2022). High Code Density and Humidity Sensor Chipless RFID Tag. 10.23919/SpliTech55088.2022.9854366.
- [29] Gao, Yuan & Mahmoodi, Mahboobeh & Zoughi, Reza. (2022). Design of a Novel Frequency-Coded Chipless RFID Tag. *IEEE Open Journal of Instrumentation and Measurement*. 1. 1-1. 10.1109/OJIM.2022.3175249.
- [30] M. Tanzeel Khalid, A. Habib, M. Nadeem, Mir Yasir Umair, Nimra Javed, (2022). "Printed humidity sensor for low-cost item tagging", *AEU - International Journal of Electronics and Communications*, Volume 157, 154441, ISSN 1434-8411, <https://doi.org/10.1016/j.aeue.2022.154441>.
- [31] Z. Xiao et al., (2015). "An implantable RFID sensor tag toward continuous glucose monitoring," *IEEE J. Biomed. Health Inf.*, vol. 19, no. 3, pp. 910–919.
- [32] Ali S, Qaisar S, Saeed H, et al. (2015), "Network challenges for cyber physical systems with tiny wireless devices: A case study on reliable pipeline condition monitoring." *Sensors*, 15(4): 7172-7205.

- [33] Lyu S, Zhang Y, Wang W, et al. (2019), “Simulation Study on Influence of Natural Gas Pipeline Pressure on Jet Fire//IOP Conference Series”, Earth and Environmental Science. IOP Publishing, 242(2): 022041.
- [34] Bui X N, Nguyen H, Le H A, et al., (2019). “Prediction of blast-induced air overpressure in open-pit mine: assessment of different artificial intelligence techniques”. Natural Resources Research, 2019: 1-21.
- [35] Abdulkawi, Wazie & Sheta, Abdel Fattah & Issa, Khaled & Alshebeili, Saleh. (2019). Compact Printable Inverted-M Shaped Chipless RFID Tag Using Dual-Polarized Excitation. Electronics. 8. 580. 10.3390/electronics8050580.
- [36] Salmerón JF, Albrecht A, Kaffah S, Becherer M, Lugli P, Rivadeneyra A., (2018). “Wireless chipless system for humidity sensing”. Sensors (Basel);18(7):2275. <https://doi:10.3390/s18072275>
- [37] Javed N, Habib A, Amin Y, Loo J, Akram A, Tenhunen H., (2016). “Directly printable moisture sensor tag for intelligent packaging”. IEEE Sens. J.;16(16):6147-48. <https://doi:10.1109/JSEN.2016.2582847>
- [38] Kapton®HN Polyimide Film Datasheet. Available online: http://www2.dupont.com/Kapton/en_US/ (accessed on 18 September 2011).
- [39] Habib S, Ali A, Kiani GI, Ayub W, Abbas SM, Butt MFU (2021). “A low-profile FSS-based high capacity chipless RFID tag for sensing and encoding applications”. International Journal of Microwave and Wireless Technologies 1–9. <https://doi.org/10.1017/S1759078721000362>
- [40] http://cgtec.eu/wp-content/uploads/Stanyl_brochure_02.pdf
- [41] Vena, A.; Perret, E.; Tedjini, S., (2011). “Chipless RFID tag using the hybrid coding technique”. IEEE Trans. Microw. Theory Technol. 59(12), 3356–3364.

- [42] M. Polivka, M. Svanda, J. Havlicek, and J. Machac, (2017). “Detuned dipole array backed by rectangular plate applied as chipless RFID tag,” in Proc. Prog. Electromagn. Res. Symp.-Spring (PIERS), St. Petersburg, Russia, , pp. 3314–3317, doi: 10.1109/PIERS.2017.8262328.
- [43] Shahid H, Riaz MA, Akram A, Amin Y Loo J et al., (2019). “Novel QR-incorporated hipless RFID tag”. IEIC Electron; 16: 20180843-20180843.
- [44] Abdulkawi, Wazie & Sheta, Abdel Fattah & Issa, Khaled & Alshebeili, Saleh. (2019). Compact Printable Inverted-M Shaped Chipless RFID Tag Using Dual-Polarized Excitation. Electronics. 8. 580. 10.3390/electronics8050580.
- [45] Jabeen, Iqra & Ejaz, Asma & Akram, Adeel & Amin, Y. & Loo, Jonathan & Tenhunen, Hannu & Amin, Y.. (2019). Elliptical slot based polarization insensitive compact and flexible chipless RFID tag. International Journal of RF and Microwave Computer-Aided Engineering. 10.1002/mmce.21734.
- [46] T. Athauda and N. C. Karmakar, (2019). “The realization of chipless RFID resonator for multiple physical parameter sensing,” IEEE Internet Things J., vol. 6, no. 3, pp. 5387–5396.
- [47] Tariq N, Riaz MA, Shahid H, Khan MJ, Khan MS, Amin Y, Loo J and Tenhunen H (2019) Orientation independent chipless RFID tag using novel trefoil resonators. IEEE Access 7, 122398–122407
- [48] N. Chen, Y. Shen, G. Dong and S. Hu, (2019). "Compact Scalable Modeling of Chipless RFID Tag Based on High-Impedance Surface," in IEEE Transactions on Electron Devices, vol. 66, no. 1, pp. 200-206. doi: 10.1109/TED.2018.2864623.
- [49] Shahid L, Shahid H, Riaz MA, Naqvi SI, Jamil M et al. (2019). “Chipless RFID tag for touch event sensing and localization.”, IEEE Access.

- [50] Jabeen, I.; Ejaz, A.; Rehman, M.; Naghshvarianjahromi, M.; Khan, M.; Amin, Y.; Loo, J.; Tenhunen, H, (2019), “Data-dense and miniature Chipless moisture sensor RFID tag for Internet of Things. *Electronics*;, 8(10), 1182. <https://doi.org/10.3390/electronics810118>
- [51] Chen YS, Jiang TY and Lai FP (2019) Design rule development for frequency-coded chipless radiofrequency identification with high capacity. *IET Microwaves Antennas & Propagation* 13, 1255–1261.
- [52] M. S. Hashmi and V. Sharma (2020), “Design, analysis, and realization of chipless RFID tag for orientation independent configurations”, *Eng. J.*, vol. 2020, no. 5, pp. 189–196.

LIST OF PUBLICATIONS

- [1] M. Tanzeel Khalid, A. Habib, M. Nadeem, Mir Yasir Umair, Nimra Javed, (2022). "Printed humidity sensor for low-cost item tagging", *AEU - International Journal of Electronics and Communications*, Volume 157, 154441, ISSN 1434-8411, <https://doi.org/10.1016/j.aeue.2022.154441>.
- [2] Habib and M. Nadeem, "Multi-resonator Based Passive Chipless RFID Tag for Tracking Applications," *2023 International Conference on Communication Technologies (ComTech)*, Rawalpindi, Pakistan, 2023, pp. 69-72, doi: 10.1109/ComTech57708.2023.10165189.